

TRESK background potassium channel regulates MrgprA3⁺ pruriceptor excitability, acute and chronic itch

Júlia Llimós-Aubach^{a,b}, Alba Andres-Bilbe^{a,b}, Anna Pujol-Coma^{a,b}, Aida Castellanos^{a,b}, Irene Pallás^{a,b}, Maria Isabel Bahamonde^{a,b}, Josep Maria de Anta^c, Concepció Soler^{c,d}, Núria Comes^{a,b}, Gerard Callejo^{a,b}, Xavier Gasull^{a,b,*}

Abstract

A subset of peripheral sensory neurons expressing specific Mas-related G-protein-coupled receptors and transient receptor potential channels mediate pruritogen-induced chemical itch. However, the molecular mechanisms that regulate the excitability of these cells, and consequently itch sensation, are poorly understood. TWIK-related spinal cord K⁺ channel (TRESK) is a background K⁺ channel that modulates the resting membrane potential, action potential firing, and neuronal excitability, and it has been involved in somatosensation and pain transduction. Here, we demonstrate that this channel contributes to pruritic transduction and it is a potential target for treating chronic itch pathologies. TRESK channel coexpress with Mas-related G-protein-coupled receptor A3, MrgprC11 and MrgprD in mouse sensory neurons, and with MrgprX1 in human ones. Genetic ablation of TRESK enhances firing of MrgprA3-expressing pruriceptors and acute itch in response to intradermal injection of chloroquine, while the response to histamine, BAM8-22, or leukotriene C4 remains unaffected. TRESK deletion also exacerbates chronic itch in mouse models of allergic contact dermatitis, dry skin, and imiquimod-induced psoriasiform dermatitis, resulting in a significantly increased scratching behavior that develops earlier and is more robust. Moreover, pharmacologically enhancing TRESK function diminishes both acute and chronic itch in wild-type mice but not in TRESK knockout (KO) animals. In summary, our data indicate that TRESK plays a role in regulating the excitability of a subset of sensory neurons that mediate histaminergic-independent itch. Enhancing the channel function with specific activators represents a promising antipruritic therapeutic approach that can be combined with other compounds for the treatment of nonhistaminergic itch, which currently lack adequate treatment options.

Keywords: Nociceptor, pruriceptor, K2P channels, itch, skin disease, chronic itch, sensory neuron excitability, chloroquine, nonhistaminergic itch

1. Introduction

Itch is an unpleasant sensation that triggers a desire to scratch and is considered a warning sign aimed to remove possible irritants or harmful stimuli. Pathologically, chronic itch is associated with many skin (atopic dermatitis, psoriasis, dry skin) and systemic diseases (cholestasis, chronic kidney disease).^{19,35} In rodents, 3 subpopulations of nonpeptidergic (NP) sensory neurons involved in itch sensing have been described by genetic

and functional approaches^{7,35,58}: NP1, presenting distinctive expression of Mas-related G-protein-coupled receptor D (MrgprD); NP2, expressing MrgprA3 and MrgprC11; and NP3, expressing histamine and serotonin receptors.^{10,16,23,29,73} Other itch receptors such as PAR2, interleukins, or thymic stromal lymphopoietin are also expressed in these neurons.^{7,10,18,61,63} In humans, similar populations of pruriceptors exist containing the

Sponsorships or competing interests that may be relevant to content are disclosed at the end of this article.

G. Callejo and X. Gasull are senior authors.

X. Gasull lead contact.

J. Llimós-Aubach and A. Andres-Bilbe contributed equally to this work.

^a Neurophysiology Laboratory, Department of Biomedicine, Medical School, Institute of Neurosciences, Universitat de Barcelona, Barcelona, Spain, ^b Institut d'Investigacions Biomèdiques August Pi i Sunyer (IDIBAPS), Barcelona, Spain, ^c Department of Pathology and Experimental Therapy, School of Medicine, Universitat de Barcelona, Barcelona, Spain, ^d Immunity, Inflammation and Cancer Group, Oncobell Program, Institut d'Investigació Biomèdica de Bellvitge-IDIBELL, Barcelona, Spain

*Corresponding author. Address: Department Biomedicina-Fisiologia, Facultat de Medicina, Universitat de Barcelona, Casanova 143, Barcelona E-08036, Spain. E-mail address: xgasull@ub.edu (X. Gasull)

Supplemental digital content is available for this article. Direct URL citations appear in the printed text and are provided in the HTML and PDF versions of this article on the journal's Web site (www.painjournalonline.com).

Copyright © 2025 The Author(s). Published by Wolters Kluwer Health, Inc. on behalf of the International Association for the Study of Pain. This is an open access article distributed under the terms of the Creative Commons Attribution-Non Commercial-No Derivatives License 4.0 (CCBY-NC-ND), where it is permissible to download and share the work provided it is properly cited. The work cannot be changed in any way or used commercially without permission from the journal.

<http://dx.doi.org/10.1097/j.pain.0000000000003540>

same itch receptors or human orthologs (MrgprX1 in humans is a functional homolog to MrgprA3 and MrgprC11 in rodents). Nevertheless, in humans, the difference between peptidergic and NP sensory neurons subtypes is more diffuse and pruriceptors also express several neuropeptides.^{46,53}

The intensity of pruriceptors' activation by different stimuli is directly related to the sensation of itch and beyond the membrane receptors activated by pruritogens, ion channels such as TRPV1, TRPA1, or ANO1 appear to play a role in the transduction pathway, leading to neuronal depolarization and initiation of action potentials firing.^{18,21,33,61} Interestingly, in MrgprA3-expressing neurons, different transduction pathways can induce either itch or pain, depending on the activation of metabotropic or ionotropic membrane receptors, respectively.⁴⁴ In addition, gain-of-function mutations on Na_v1.9 (SCN11A) cause a pruritic phenotype in mice and severe pruritus in humans, which has been associated with its high expression in itch nociceptors.⁴³ These findings suggest that each neuronal subtype presents a characteristic pattern of ion channel expression, defining their intrinsic physiological properties, activation mechanism, AP characteristics, and firing pattern.⁷⁰

Two-pore domain potassium channels are expressed in different sensory neuron subpopulations, including nociceptors, where they predominantly carry "leak" or background hyperpolarizing current.¹¹ Their electrophysiological properties allow them to carry K⁺ currents across a broad range of membrane potentials, positioning them as crucial regulators of neuronal excitability. This is achieved by decreasing the likelihood of depolarizing stimuli reaching AP threshold and shaping the neuron firing response.¹¹ In humans and rodents, TWIK-related spinal cord K⁺ channel (TRESK) exhibit high expression in neurons of the trigeminal (TG) and dorsal root ganglion (DRG).^{6,20,31,58,68} We showed that genetic ablation of TRESK enhances mechanical and cold sensitivity, whereas sensitivity to heat remains largely unaffected.^{1,6} In addition, mutations in the channel have been linked to migraine pain.^{22,36,40}

As transcriptomic analyses revealed that TRESK exhibits preferential expression in NP1 and NP2 subtypes of sensory neurons that are implicated in itch signal transmission,^{8,12,30,38,58,68} we investigated whether the channel could contribute to regulating pruriceptor excitability and if changes in its expression or function might cause persistent activation of pruriceptors, leading to chronic itch. We show that TRESK is a key regulator of nonhistaminergic itch and manipulating its function emerges as a promising novel approach for antipruritic therapy.

2. Methods

2.1. Animals

All behavioral and experimental procedures were conducted in accordance with the recommendations of the International Association for the Study of Pain and were reviewed and approved by the Animal Care Committee of the University of Barcelona and by the Department of the Environment of the Generalitat de Catalunya, Catalonia, Spain (#9876, 10191, 10326). Female and male C57BL/6 mice between 8 and 16 weeks old were used in all experimental procedures (RNA extraction and qPCR, in situ hybridization [ISH], cell cultures, electrophysiology, calcium imaging, and behavior) unless specified otherwise. Mice were kept in a controlled environment at 22°C with unrestricted access to food and water in a 12-hour alternating light and dark cycle.

TRESK channel (Kcnk18/K2P18.1) knockout mice (KO) and wild-type (WT) littermates were obtained from the KOMP Repository (Mouse Biology Program, University of California, Davis, CA). The TRESK knockout mouse was generated by replacing the complete Kcnk18 gene by a ZEN-UB1 cassette according to the VelociGene's KOMP Definitive Null Allele Design. At 3 weeks of age, WT or KO newborn mice were weaned, separated, and identified by ear punching. Genomic DNA was isolated from ear snip samples incubated in a solution containing 25 mM NaOH and 0.2 mM EDTA (pH 12) at 95°C during 30 minutes, after neutralization with 40 mM Tris-HCl solution at pH 5. Polymerase chain reaction (PCR) was performed with primers to detect the Kcnk18 gene: forward 5'-GGAGAACCC TGAGTTGAAGAAGTTCC-3' and reverse GGCTCTAACTTTCCT CACTGCACC or the inserted cassette in the KO mice: forward (REG-Neo-F) GCAGCCTCTGTCCACATACACTTCA and reverse (gene-specific) AGACTTCTCCCAGGTAACAACACTCTGC. The PCR mixture contained 9 μL DNA sample, 10 μL Master Mix (ThermoFisher Scientific, Waltham, MA; Ref. K0171), 0.5 μL (20 μM) forward and reverse primers (final volume of 20 μL). Polymerase chain reaction amplifications were conducted with 35 cycles in a programmable thermal cycler (Eppendorf AG, Hamburg, Germany). The program used was 95°C for 3 minutes and cycles of 95°C for 30 seconds, 58°C for 60 seconds, 72°C for 40 seconds, with a final extension at 72°C for 5 minutes. Polymerase chain reaction products were analyzed by electrophoresis in 1.5% agarose gels. Once identified, genotyped animals were used as breeders for colony expansion and their offspring were used in all experimental procedures in which mice were required. The transgenic MrgprA3^{GFP-Cre} mouse (Tg(Mrgpra3-GFP/cre)) line was kindly provided by Mark Hoon (NIH, Bethesda, MD) and Xinzhong Dong (Johns Hopkins University, HHMI)¹⁶ and crossed with a Cre-dependent ROSA26^{tdTomato} reporter mouse line (Gt(ROSA)26Sortm14(-GAG-tdTomato)Hze) providing the expression and of tdTomato in MrgprA3-expressing neurons in the resulting mouse line (MrgprA3^{tdTomato}). This MrgprA3^{tdTomato} mouse line was further crossed with TRESK^{-/-} mice to obtain the MrgprA3^{tdTomato}; TRESK^{-/-} mouse line. Primers for CRE recombinase (Cre-F: CAGAGACGGAAATCCATCGC; Cre-R: GGTGCAAGTTGAATA ACCGG), Gt(ROSA) WT (forward: GGCATTAAGCAGCGTAT CC; reverse: CTGTTCCCTGTACGGCATGG), and Gt(ROSA) Mut (forward: AAGGGAGCTGCAGTGGAGTA; reverse: CCGAAA ATCTGTGGGAAGTC) were used. The program for the Cre PCR used was 95°C for 3 minutes and cycles of 95°C for 30 seconds, 53°C for 60 seconds, 72°C for 30 seconds, with a final extension at 72°C for 5 minutes. The program for the Gt(ROSA) PCR used was 95°C for 3 minutes and cycles of 95°C for 30 seconds, 58°C for 60 seconds, 72°C for 30 seconds, with a final extension at 72°C for 5 minutes. Mice generated were used to obtain primary cultures of tdTomato-labeled MrgprA3⁺ sensory neurons from control or TRESK^{-/-} animals for electrophysiological recordings.

2.2. RNAscope in situ hybridization

Mouse DRGs (bilateral lumbar L2-L5) or TG tissues were dissected from WT or KO mice. Adult human fresh-frozen DRG (from thoracic level T10) tissue from a healthy donor was obtained from Anabios Corporation (San Diego, CA). Mouse TG/DRG and human DRG were embedded with OCT (optimal cutting temperature compound), cryostat-sectioned at 14 μm for mouse TG/DRGs and 20 μm for the human DRG onto SuperFrost Plus slides and then stored at -80°C for ISH. Multilabeling ISH was

performed using fresh frozen tissue with the RNAscope technology (Advanced Cell Diagnostics, Newark, CA) according to the manufacturer's instructions. Probes against mouse *Mm-kcnk18* (TRESK, 440001), *Mm-mrgpra3* (MAS-related GPR family member A3, 548161), *Mm-mrgprx1* (MAS-related GPR family member X1(C11), 488771), *Mm-mrgprD* (MAS-related GPR family member D, 417921), *Mm-tubb3* (Tubulin beta 3, 423391) and human *Hs-kcnk18* (TRESK, 596461), *Hs-mrgprX1* (MAS-related GPR family member X1, 517011), *Hs-tubb3* (Tubulin beta 3, 318901) mRNAs (Bio-Techne R&D Systems, S.L.U, Minneapolis, MN) were used in conjunction with the RNAscope multiplex fluorescent v2 development kit (ACD). Images were obtained on a Zeiss LSM880 confocal laser-scanning microscope (Jena, Germany) and Thunder Leica widefield fluorescence microscope. ImageJ Fiji (NIH) was used to analyze images and to determine soma size.

2.3. RNA extraction and quantitative real-time polymerase chain reaction

Mouse tissue samples were obtained from TG at indicated times, kept in RNAlater solution (Qiagen, Madrid, Spain), frozen in liquid N₂ and stored at -80°C until use. Total RNA was isolated using the Nucleospin RNA (Macherey-Nagel, Düren, Germany) and quantified for purity in a Nanodrop (ThermoFisher Scientific). First-strand cDNA was then transcribed using the SuperScript IV Reverse Transcriptase (Invitrogen, Waltham, MA; ThermoFisher Scientific) according to the manufacturer's instructions. Quantitative real-time PCR was performed in an ABI Prism 7300 using the Fast SYBR Green Master mix (Applied Biosystems, Waltham, MA) and primers (detailed below) obtained from Invitrogen (ThermoFisher Scientific). Amplification of glyceraldehyde 3-phosphate dehydrogenase transcripts was used as a standard for normalization of all qPCR experiments, and gene-fold expression was assessed using the ΔC_T method. All reactions were performed in triplicate. After amplification, melting curves were obtained and evaluated to confirm correct transcript amplification. Gene-specific primers used were *tresk* (forward 5'-CTCTCTTCTCCGCTGTCGAG-3'; reverse 5'-AAGAGAGCGCTCAGGAAGG-3'); *mrgpra3* (forward 5'-CTCAAGTTTACCCTA CCCAAAGG-3'; reverse 5'-CCGCAGAAATAACCATCCAGAA-3'); *mrgprD* (forward 5'-TTTTTCAGTGACATTCCTCGCC-3'; reverse 5'-GCACATAGACACAGAAGGGAGA-3'); *mrgprC11* (forward 5'-ACTCTCTGCTACGGATCATTGA-3'; reverse 5'-TGA TTGCTGCATTGCCTAAGATA-3'); *tpa1* (forward 5'-GTCCAG GGCGTTGTCTATCG-3'; reverse 5'-CGTGATGCAGAGGAC AGAGAT-3'); *tpv1* (forward 5'-CCCAGGAAGACAGATAGCC TGA-3'; reverse 5'-TTCAATGGCAATGTGTAATGCTG-3'); *gapdh* (forward 5'-TCCACTGGCGTCTTCAC-3'; reverse 5'-GGCAGAGATGATGACCCTTTT-3').

2.4. Primary culture of sensory neurons

Mice were humanely euthanized through cervical dislocation and decapitation under isoflurane anesthesia. Trigeminal ganglia were dissected for neuronal culture as previously described.^{5,6} Briefly, the collected ganglia were maintained in cold (4-5°C) Ca²⁺- and Mg²⁺-free phosphate buffered saline (PBS) solution supplemented with 10 mM glucose, 10 mM HEPES, 100 U.I./mL penicillin, and 100 µg/mL streptomycin until dissociation. Subsequently, ganglia were incubated in 2 mL HAM F-12 with collagenase CLS I (1 mg/mL; Biochrome AG, Berlin, Germany), Bovine Serum Albumin (1 mg/mL), and dispase II (5 mg/mL; Sigma-Aldrich, Madrid, Spain) for 1 hour

45 minutes at 37°C followed. Ganglia were then resuspended in culture media (HAM F-12 supplemented with 10% fetal bovine serum (FBS), 100 µg/mL of penicillin/streptomycin and 100 mg/mL of L-glutamine) and mechanical dissociation was conducted with fire-polished glass Pasteur pipettes of decreasing diameters, previously coated with Sigmacote (Sigma-Aldrich) and autoclaved. The resulting neurons were centrifuged at 1000 revolutions per minute (rpm) for 5 minutes, resuspended in culture medium, and transferred to 12-mm diameter glass coverslips pretreated with poly-L-lysine/laminin. The primary cultures were then incubated at 37°C in humidified 5% CO₂ atmosphere and used between 4 and 24 hours for patch-clamp electrophysiological recordings or calcium imaging experiments.

2.5. Calcium imaging in sensory neurons

Cultured trigeminal sensory neurons from WT and TRESK KO mice were loaded with 5 µM fura-2/AM (F1221; Invitrogen, ThermoFisher Scientific) for 45 to 60 minutes at 37°C in culture medium. Coverslips with fura-2 loaded cells were transferred into an open-flow chamber (0.5 mL) mounted on the stage of an inverted Olympus IX70 microscope equipped with a Lambda 721 Optical Beam combiner equipped with LEDs (Sutter Instrument, Novato, CA) as a source of illumination. Pictures were acquired with an attached cooled CCD camera (Orca-Fusion; Hamamatsu Photonics, Shizuoka, Japan) and stored and analyzed on a PC computer using HCLImage software (Hamamatsu Photonics). After a stabilization period, pairs of images were obtained every 2 seconds at excitation wavelengths of 340 (λ₁) or 380 nm (λ₂; 10 nm bandwidth filters) to excite the Ca²⁺ bound or Ca²⁺ free forms of the fura-2 dye, respectively. The emission wavelength was 510 nm (12-nm bandwidth filter). Typically, 30 to 50 cells were present in the microscope field (20x). [Ca²⁺]_i values were calculated and analyzed individually for each single cell from the 340- to 380-nm fluorescence ratios at each time point. Only neurons that produced a response >20% of the baseline value and that, at the end of the experiment, produced a Ca²⁺ response to ionomycin (1 µM) application were included in the analysis. Trigeminal neurons recorded were obtained from 4 to 5 different animals per genotype and used 18 to 24 hours after primary culture. The extracellular (bath) solution used was Hank's Balanced Salt Solution: 140 mM NaCl, 4 mM KCl, 1.8 mM CaCl₂, 1 mM MgCl₂, 10 mM glucose, 10 mM HEPES, at pH 7.4 with NaOH. Experiments were performed at room temperature. Drugs were bath-applied for 30 seconds and then washed out.

2.6. Calcium imaging in transfected cells

HEK293T cells, cultured in (Dulbecco's Modified Eagle Medium) DMEM supplemented with 10% FBS, 100 µg/mL penicillin/streptomycin, and 100 mg/mL L-glutamine at 37°C in humidified 5% CO₂, were seeded on 12-mm diameter poly-L-lysine coated glass coverslips 24 hours before transfection. Cells were transiently transfected using ROTIFect transfection reagent (Carl Roth, Karlsruhe, Germany), according to the manufacturer's instructions. *Mrgpra3*-pcDNA3.1 was kindly provided by X. Dong (Johns Hopkins University, HHMI). Human TRESK (kindly provided by Y. Sano, Astellas Pharma, Tokyo, Japan) was subcloned into the pIRES2-EGFP vector (Clontech, Mountain View, CA) to form the hTRESK-pIRES2-EGFP construct. Cells were cotransfected with *Mrgpra3*-pcDNA3.1 and pIRES2-EGFP (5:1 ratio) to allow identification of transfected cells or with *Mrgpra3*-pcDNA3.1 and hTRESK-pIRES2-EGFP (5:1 ratio). Cells were

used 24 hours later for calcium imaging with Fura-2 using the same solutions and methods as described for sensory neurons. Chloroquine (CQ) 1 mM was used to stimulate the MrgprA3 receptor.

2.7. Electrophysiological recordings

Electrophysiological recordings in sensory neurons were performed as previously described.^{4–6} Briefly, recordings were performed with a patch-clamp amplifier (Axopatch 200B; Molecular Devices, Union City, CA) and restricted to tdTomato-expressing TG neurons from MrgprA3^{TdTomato} or MrgprA3^{TdTomato}; TRESK^{-/-} mice, which had a soma diameter <30 μm and largely correspond to nociceptive/pruriceptive neurons.²⁵ Patch electrodes were fabricated in a Flaming/Brown micropipette puller P-97 (Sutter instrument). Electrodes had a resistance between 2 and 4 M Ω when filled with intracellular solution (in millimolar): 30 KCl, 110 K-Gluconate, 2 MgCl₂, 10 HEPES, adjusted to pH 7.2. Bath solution (in millimolar): 145 NaCl, 5 KCl, 2 CaCl₂, 2 MgCl₂, 10 HEPES, 5 glucose at pH 7.4. The osmolality of the isotonic solution was 310.6 \pm 1.8 mOsm/kg. To study sensory neuron excitability, after achieving the whole-cell configuration of the patch-clamp technique, the amplifier was switched to current-clamp bridge mode. Recorded signals were filtered at 2 kHz, digitized at 10 kHz, and acquired with pClamp 10 software. Data were analyzed with Clampfit 10 (Molecular Devices) and Prism 10 (GraphPad Software, Inc, La Jolla, CA). Series resistance was always kept below 15 M Ω and compensated at 70% to 80%. All recordings were done 4 to 6 hours after dissociation at room temperature (22–23°C) rather than body temperature to permit direct comparisons to other studies of underlying biophysical mechanisms. Only neurons with a resting membrane voltage below –45 mV were considered for the study. Rheobase was determined with ascending series of 200 ms depolarizing pulses (10 pA increments from –50 pA) while the neuron was held at its resting membrane potential (RMP). Action potential (AP) properties (amplitude, duration, time to AP peak) were measured at the spike fired at the rheobase current. Membrane input resistance (I_r) was measured at the –50 pA current pulse. Neuronal depolarization to subthreshold stimuli (+10 pA and +20 pA) was measured to assess the contribution of potassium currents in the range of membrane potentials between resting and AP threshold. Intrinsic neuronal excitability to injected current was measured as the number of spikes during a 1 second depolarizing ramp from 0 to 500 pA. Neuronal excitability to a pruritogenic stimulus was measured as the number of spikes fired in response to bath application of CQ (1 mM) for 20 seconds.

2.8. Histology

To evaluate the skin lesions produced by the imiquimod (IMQ)-induced psoriatic skin model in WT and TRESK KO animals, a new batch of animals were treated as described in section 2.11 and sacrificed at day 4. Cheek skin specimens were dissected immediately after animals were sacrificed and fixed in 4% paraformaldehyde in Ca²⁺/Mg²⁺-free PBS and processed for paraffin embedding. Five micrometer thick sections were stained with hematoxylin and eosin. Images were obtained in a bright-field Nikon Eclipse E-800 microscope at 20x, and main histological parameters from at least 4 sections of each mouse were analyzed with ImageJ software (NIH) in a blinded manner by 2 researchers. In particular, epidermal thickness was measured

in μm and as the number of epidermal cell layers, hypergranulosis (thickness of the stratum granulosum) was assessed as a percentage of epidermal length with 2 or more epidermal granular layers, and microabscesses were quantified as the number per epidermal length.

2.9. Behavioral studies

Female and male WT or TRESK KO mice aged between 8 and 16 weeks were used in all behavioral studies. To mitigate stress-induced variability in the results, mice were acclimated to the experimental room and the experimental setup before testing (2h). Behavioral measurements were conducted in a quiet environment, with careful attention to minimize or prevent any distress of the animals. All experimenters were blind to the genotype, or the drug/vehicle assayed.

2.10. Cheek assay of acute itch

To assess acute itch sensitivity, we used the cheek assay, which allows to differentiate between itch and pain responses to a substance.⁴⁷ Mice were acclimated to the experimental room for 2 hours 1 day before testing. Compounds were intradermally injected into the cheek of the animal (10 μL). A characteristic scratching response with the posterior leg is indicative of itch while a wipe with the anterior leg indicates pain, as the animal attempts to eliminate the painful stimulus. The number of scratching bouts towards the injection site during 15-minute period was counted. In experiments using cloxyquin or olive oil (vehicle), animals received an intraperitoneal injection of the drug (50 mg/kg) 2 hours before testing.

2.11. Imiquimod-induced psoriasis model of chronic itch

The IMQ model of psoriatic itch⁴² was performed as described, on the mouse cheek. Briefly, on the day before the treatment and under short anesthesia with 2% isoflurane, the mouse's cheek skin was shaved (0.5 \times 0.5 cm). For 7 consecutive days (days 0–6), mice received a daily topical application of 12.5 mg Aldara cream (5% IMQ; 3M Pharmaceuticals, Northridge, CA) on the shaved cheek skin. Control mice was treated similarly with a control vehicle cream (Vaseline Lanette, Bioglan AB, Malmö, Sweden). The behavior of each mouse was recorded during 1 hour on day 0 (baseline, before applying any treatment), on days 1 to 6 (before IMQ reapplication), and on day 7. Animals were observed individually in its home cage where they could move freely without any type of restriction. The number of scratching bouts directed to the area was counted as a measure of spontaneous itch.

2.12. Dry skin model of chronic itch

The dry skin model was performed on the mouse cheek as described.⁶² Briefly, after shaving (0.5 \times 0.5 cm), the mouse cheek was treated twice daily during 5 days, with a cotton swab moistened with water (control group) or with a 1:1 mixture of acetone and ether (dry skin group) during 15 seconds. The treated cheek skin was then washed with water for 30 seconds. On day 1 (before applying any treatment) and on days 3 and 5 (after the second treatment of the day), the behavior of each mouse was individually observed while the animal freely moved in its home cage. The number of scratching bouts during a 1 hour period was counted as a measure of spontaneous itch.

2.13. Allergic contact dermatitis model of chronic itch

To induce allergic contact dermatitis, each mouse was challenged with the contact sensitizer squaric acid dibutyl ester (SADBE; 339792; Sigma-Aldrich) to elicit contact hypersensitivity.³⁷ Mice were sensitized by a topical application of 25 μL of 1% SADBE in acetone to the shaved back skin (0.5×0.5 cm) once a day for 3 consecutive days (days 0, 1, and 2). Five days later (day 5), the SADBE-treated group was challenged with a topical application of 1% SADBE to the shaved cheek skin once a day for 2 consecutive days (days 7 and 8), whereas acetone alone was used as the vehicle control. Spontaneous scratching behavior was observed for 1 hour on 3 consecutive days, before the SADBE challenge (day 7) and during the 2 days after (days 8 and 9).

2.14. Drugs

All reagents and culture media were obtained from Sigma-Aldrich unless otherwise indicated, including histamine (H7250), β -alanine (146064), CQ (C6628), BAM 8 to 22 (SML0729), and cloxyquin (C47000). N-methyl leukotriene C4 (LTC_4 ; CAY-13390) was obtained from Cayman Chemical (Ann Arbor, MI). All drugs were prepared fresh before every experimental procedure by diluting them in PBS at the desired concentration except LTC_4 that was diluted in PBS from a stock solution in ethanol. Cloxyquin was diluted and injected intraperitoneally in olive oil.⁶⁹ For cheek injection, cloxyquin was diluted in 1% DMSO/PBS or in olive oil.

2.15. Data analysis

Data are presented as mean \pm SEM. Statistical differences between different sets of data were assessed by performing unpaired Student *t*-tests, one-way or 2-way analysis of variance plus Bonferroni or Holm-Šidák multiple comparisons tests, as indicated. The significance level was set at $P < 0.05$ in all statistical analyses. Data analysis was performed using GraphPad Prism 10 software and GraphPad QuickCalcs online tools (GraphPad Software, Inc).

3. Results

3.1. TRESK colocalizes in sensory neuron subpopulations involved in itch signaling

Single-cell transcriptomic studies of both trigeminal and dorsal root ganglia have revealed predominant TRESK expression in specific sensory neuronal subtypes^{8,24,30,38,58,68} and particularly enriched in MrgprA3⁺ neurons.⁶⁶ The channel is expressed in low-threshold mechanoreceptors involved in touch sensation (NF1; expressing TrkB and Piezo2) but predominantly in NP nociceptors subpopulations NP1 and NP2, responsible for itch transduction. To validate these findings, we performed ISHs and quantified the coexpression percentage of TRESK with known markers of these subpopulations, MrgprD for NP1 or MrgprA3 and MrgprC11 for NP2. Trigeminal ganglia slices obtained from 3 different WT mice were assayed for *tubb3*, *kcnk18* (TRESK) and *mrgprA3*, *mrgprC11* or *mrgprD*. From 5852 neurons (*Tubb3*⁺), 2129 were positive for TRESK ($35.6 \pm 6.7\%$) and 305 for MrgprA3 ($4.9 \pm 1.5\%$), mostly being small or medium-sized neurons (**Figs. 1A and B**). A significant percentage of MrgprA3⁺ neurons ($67.9 \pm 24.3\%$, 196 neurons) exhibited a notable degree of TRESK coexpression (**Fig. 1A**). In situ hybridization from TRESK KO animals did not show any significant staining for the channel

(Suppl Fig. 1A, <http://links.lww.com/PAIN/C222>). Similar results were found in DRGs, where $57.9 \pm 4.8\%$ MrgprA3⁺ neurons express TRESK (MrgprA3⁺, 85 neurons, TRESK⁺ 642 neurons, *Tubb3*⁺, 1865 neurons; **Figs. 1A and B**). MrgprC11 showed a similar degree of colocalization with TRESK in TG neurons. From 2999 neurons (*Tubb3*⁺), 904 were positive for TRESK ($29.6 \pm 3.0\%$) and 188 for MrgprC11 ($6.8 \pm 1.5\%$), with $80.6 \pm 7.0\%$ of neurons (148) showing both TRESK and MrgprC11 coexpression (**Fig. 1C**). TWIK-related spinal cord K⁺ channel also showed a high percentage of expression in a different population of TG and DRG neurons, characterized by MrgprD⁺ expression. A $60.2 \pm 2.4\%$ of MrgprD⁺ trigeminal neurons express the ion channel (MrgprD⁺, 962 neurons, TRESK⁺ 2789 neurons, *Tubb3*⁺, 7645 neurons; **Fig. 1C**). In DRGs, the percentage of MrgprD⁺ neurons expressing the channel was slightly higher ($73.2 \pm 6.2\%$; MrgprD⁺, 1064 neurons, TRESK⁺ 1509 neurons, *Tubb3*⁺, 4590 neurons; Suppl Fig. 1B, <http://links.lww.com/PAIN/C222>). Therefore, ISH data confirm transcriptomic studies, showing that TRESK is highly expressed in NP1 and NP2 neuronal subtypes involved in itch transduction. Next, we assayed whether TRESK was also present in human DRG sensory neurons expressing MrgprX1, the human analog of MrgprA3, and if they present a similar expression pattern. As shown in **Figure 1D**, a similar degree of coexpression was found, with $96.9 \pm 1.9\%$ of MrgprX1⁺ neurons presenting TRESK expression (MrgprX1⁺, 76 neurons, TRESK⁺ 142 neurons, *Tubb3*⁺, 502 neurons; **Fig. 1D**). These data confirm that pruriceptors expressing Mrgpr receptors coexpress TRESK channels in both species, humans, and rodents.

3.2. TRESK ablation enhances acute itch

Considering the role of TRESK regulating neuronal excitability^{6,36,40,60} and its expression in pruriceptors, we reasoned that the absence of the channel could heighten neuronal activation by pruritogenic compounds. To test this hypothesis, we used the cheek assay⁴⁷ to assess itch responses after the injection of different well-known pruritogens in WT and TRESK KO mice. As anticipated, CQ injection (50 μg in 10 μL), a MrgprA3 agonist,²⁸ resulted in significant scratching compared to vehicle injection in both genotypes (**Fig. 2A**). Interestingly, mice lacking TRESK exhibited an augmented response to CQ (WT vs KO: 24.5 ± 13.9 vs 48.6 ± 26.6 scratching bouts; $P < 0.01$; **Fig. 2A** and Suppl Fig. 2, <http://links.lww.com/PAIN/C222>), suggesting that the absence of the channel facilitates neuronal activation. Similar results for CQ injection in the nape of the neck were found, a territory innervated by DRG neurons (WT vs KO; $P < 0.01$; **Fig. 2B**). In contrast, scratching bouts induced by cheek injection of histamine (30 μg ; activating H1R receptors), BAM8-22 (5 mM; activating MrgprC11), and N-met LTC_4 (1 μg ; activating Cys1r2) were similar between WT or KO animals, despite inducing significant scratching in all groups compared to vehicle (**Fig. 2C**). In our hands, cheek injection of β -alanine (1 mM) only produced a mild effect in both WT and KO mice (not shown) despite others have reported significant effects²⁹ or a higher concentration must be used.¹⁵ None of these compounds elicited almost any wiping responses (indicative of pain⁴⁷), thus confirming that tested compounds induced itch rather than pain. These results suggest that TRESK modulates specific populations of itch-transducing sensory neurons, preferentially nonhistaminergic itch transduction mediated by MrgprA3⁺ pruriceptors (NP2) activation. To assess if the enhanced scratching response in KO mice resulted from an increased number of neurons responding to CQ, we performed calcium imaging experiments to determine the

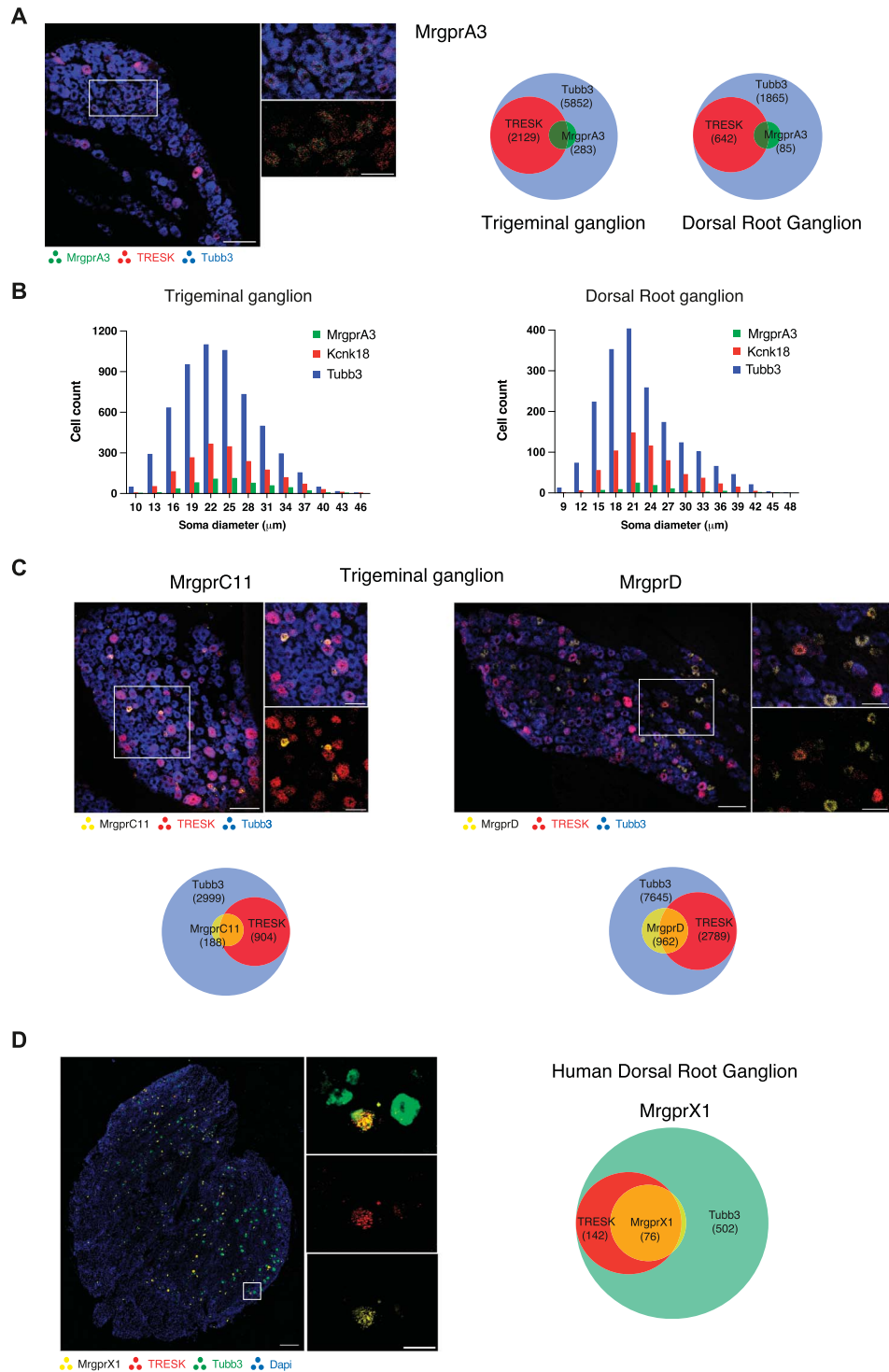


Figure 1. Coexpression of TRESK and Mrg receptors in sensory neurons. (A) *Left*, Triple-label in situ hybridization of MrgprA3 (green), TRESK (red), and tubulin beta 3 (Tubb3, blue) in the trigeminal ganglion from wild-type (WT) mouse. Detailed coexpression of MrgprA3 and TRESK can be seen in neurons (Tubb3⁺) from the inset. Scale bar: 100 µm; Inset: 50 µm. *Right*, Venn diagrams depicting the number of cells expressing MrgprA3 and TRESK in the total neuronal population (Tubb3⁺) and the overlapping mRNA expression pattern in trigeminal and dorsal root ganglia. Data were obtained from 8 to 10 sections from n = 3 to 4 mice per ganglia. (B) Quantification and distribution of soma size for the 3 groups in trigeminal and dorsal root ganglia sensory neurons, revealing that TRESK and MrgprA3 are predominantly expressed in small and medium sensory neurons. (C) *Top*, Triple-label in situ hybridization of MrgprC11 (*left*; yellow) or Mas-related G-protein-coupled receptor D (MrgprD) (*right*; yellow), TRESK (red), and tubulin beta 3 (Tubb3, blue) in the trigeminal ganglion from WT mouse. Detailed coexpression of MrgprC11 or MrgprD and TRESK can be seen in neurons (Tubb3⁺) from the inset. Scale bar: 100 µm; Inset: 50 µm. *Bottom*, Venn diagrams depicting the number of cells expressing MrgprC11 or MrgprD and TRESK in the total neuronal population (Tubb3⁺) and the overlapping mRNA expression pattern. Data were obtained from 8 to 10 sections from n = 3 to 4 mice. (D) *Left*, Triple-label in situ hybridization of MrgprX1 (yellow), TRESK (red), tubulin beta 3 (Tubb3, green) and cell nuclei (dapi, blue) in a human dorsal root ganglion. Detailed coexpression of MrgprX1, TRESK can be seen in neurons (Tubb3⁺) from the inset, as well as individually. Scale bar: 300 µm; Inset: 50 µm. *Right*, Venn diagram depicting the number of cells expressing MrgprX1 and TRESK in the total neuronal population (Tubb3⁺) and the overlapping mRNA expression pattern in dorsal root ganglia. Data were obtained from 3 different sections from a hDRG T10 ganglion. TRESK, TWIK-related spinal cord K⁺ channel.

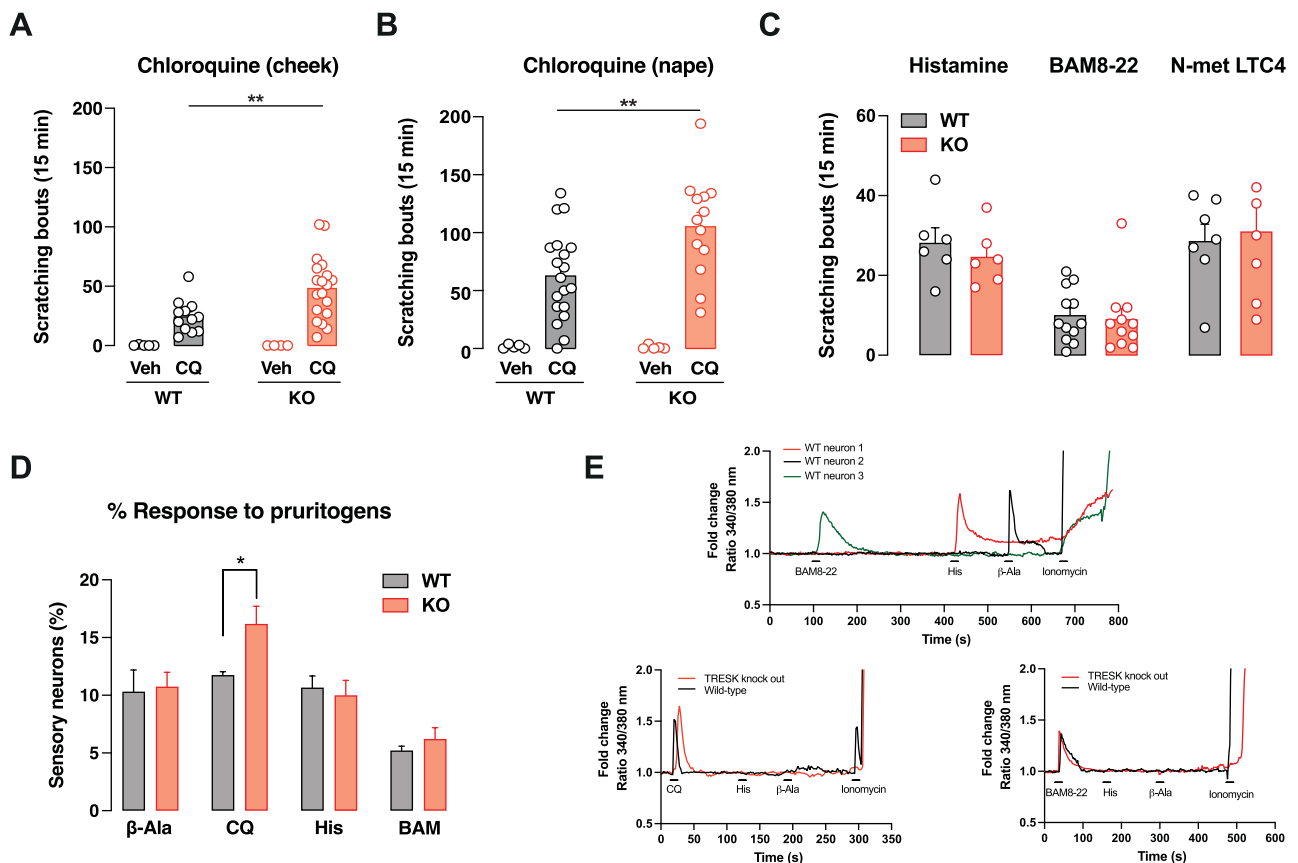


Figure 2. Deletion of TRESK enhances nonhistaminergic acute itch. (A) Intradermal injection of chloroquine (50 $\mu\text{g}/10 \mu\text{L}$; 9.7 mM; wild-type [WT] $n = 12$, knockout [KO] $n = 19$), histamine (30 $\mu\text{g}/10 \mu\text{L}$; 16.3 mM; WT, KO $n = 6$ each), BAM8-22 (50 nmol/10 μL ; 5 mM; WT $n = 8$, KO $n = 6$), or N-met leukotriene C4 (LTC4) (1 $\mu\text{g}/10 \mu\text{L}$; 0.16 mM; WT, KO $n = 7$ each) into the cheek induced acute scratching that was significantly greater than vehicle injection ($n = 4$ –5). An enhanced response was observed in TRESK KO animals in response to chloroquine compared to WT mice (** $P < 0.01$, unpaired 2-tailed Student t -test). (B) Similar results were obtained when injecting chloroquine in the nape of the neck, a territory innervated by dorsal root ganglion (DRG) sensory neurons (** $P < 0.01$, unpaired 2-tailed Student t -test). WT vehicle $n = 5$, CQ $n = 19$; KO vehicle $n = 5$, CQ $n = 13$. (C) No significant differences were observed between genotypes after cheek intradermal injection of histamine (30 $\mu\text{g}/10 \mu\text{L}$; 16.3 mM; WT, KO $n = 6$ each), BAM8-22 (50 nmol/10 μL ; 5 mM; WT $n = 8$, KO $n = 6$), or N-met LTC4 (1 $\mu\text{g}/10 \mu\text{L}$; 0.16 mM; WT, KO $n = 7$ each). (D) Percentage of neurons from WT and TRESK KO mice showing increases in intracellular calcium after challenge with the above-indicated pruritogens (β -alanine, 1 mM; chloroquine, 1 mM; histamine, 300 μM and BAM8-22, 100 μM). Trigeminal neurons from WT ($n = 943$) and TRESK KO ($n = 1500$) mice were obtained from 4 to 5 different animals per genotype and recorded 18 to 24 hours after primary culture. A significant percentage of TRESK KO neurons responded to CQ (* $P < 0.05$, unpaired 2-tailed Student t -test). (E) *Top*. Example traces of calcium experiments for the different pruritogens tested in WT trigeminal neurons. *Bottom*. Example traces of calcium peaks induced by chloroquine (left) and BAM8-22 (right) in WT and TRESK KO trigeminal neurons. CQ, chloroquine; TRESK, TWIK-related spinal cord K^+ channel.

percentage of trigeminal neurons responding to β -alanine (1 mM), CQ (1 mM), histamine (300 μM), or BAM8-22 (100 μM). No significant differences were found in the percentage of neurons activated by β -alanine (WT, 10.3%, KO 10.7%), histamine (WT, 10.6%, KO 9.9%), or BAM8-22 (WT, 5.2%, KO 6.2%; **Figs. 2D and E**) or the amplitude of the calcium peaks, indicating that neuronal populations were largely similar and unaltered in KO mice. Nevertheless, the percentage of trigeminal neurons responding to CQ in KO animals were slightly higher compared to WT (16.2% vs 11.7%, respectively; $P < 0.05$; **Fig. 2D**) but not the amplitude of the calcium peak (340/380 nm ratio fold-change, WT 1.40 ± 0.70 vs KO 1.62 ± 0.72 , $P > 0.05$). To specifically assess if the presence of TRESK modifies the calcium response to MrgprA3 activation, we evaluated CQ-mediated calcium responses in a heterologous system where other possible mechanisms are largely absent. HEK293 cells expressing MrgprA3+TRESK were activated by CQ (1 mM) and produced Ca^{2+} peaks similar to cells transfected with MrgprA3+EGFP (340/380 nm ratio fold-change: 1.44 ± 0.23 vs 1.62 ± 0.39 , respectively; $P > 0.05$; Suppl Fig. 3, <http://links.lww.com/PAIN/C222>), suggesting that the activation of MrgprA3 is independent of TRESK presence. All together indicates that the absence of

TRESK might increase the number of neurons activated and, therefore, the behavioral response associated. The percentage of neurons responding to CQ in calcium imaging experiments were slightly higher compared to the percentage of neurons MrgprA3⁺ in ISH experiments. This might be because of an overestimation of small Ca^{2+} responses or to off-target effects of CQ. Nevertheless, this is likely to occur similarly in both WT and KO neurons, allowing to compare between genotypes.

3.3. TRESK regulates MrgprA3⁺ neurons excitability

In a previous study, we observed that TRESK deletion enhanced the excitability of small and medium sensory neurons.⁶ To specifically investigate whether the absence of TRESK enhances the excitability of MrgprA3⁺ neurons, we recorded trigeminal neurons from the MrgprA3^{tdTomato}; TRESK^{+/+} ($n = 14$) and MrgprA3^{tdTomato}; TRESK^{-/-} mice ($n = 11$). As illustrated in **Figures 3A and B**, we noted significant differences in the input resistance ($P = 0.033$) and rheobase current ($P = 0.039$), while no differences were encountered for AP amplitude ($P = 0.658$) and width ($P = 0.613$), time-to-AP peak ($P = 0.729$) or afterhyperpolarization

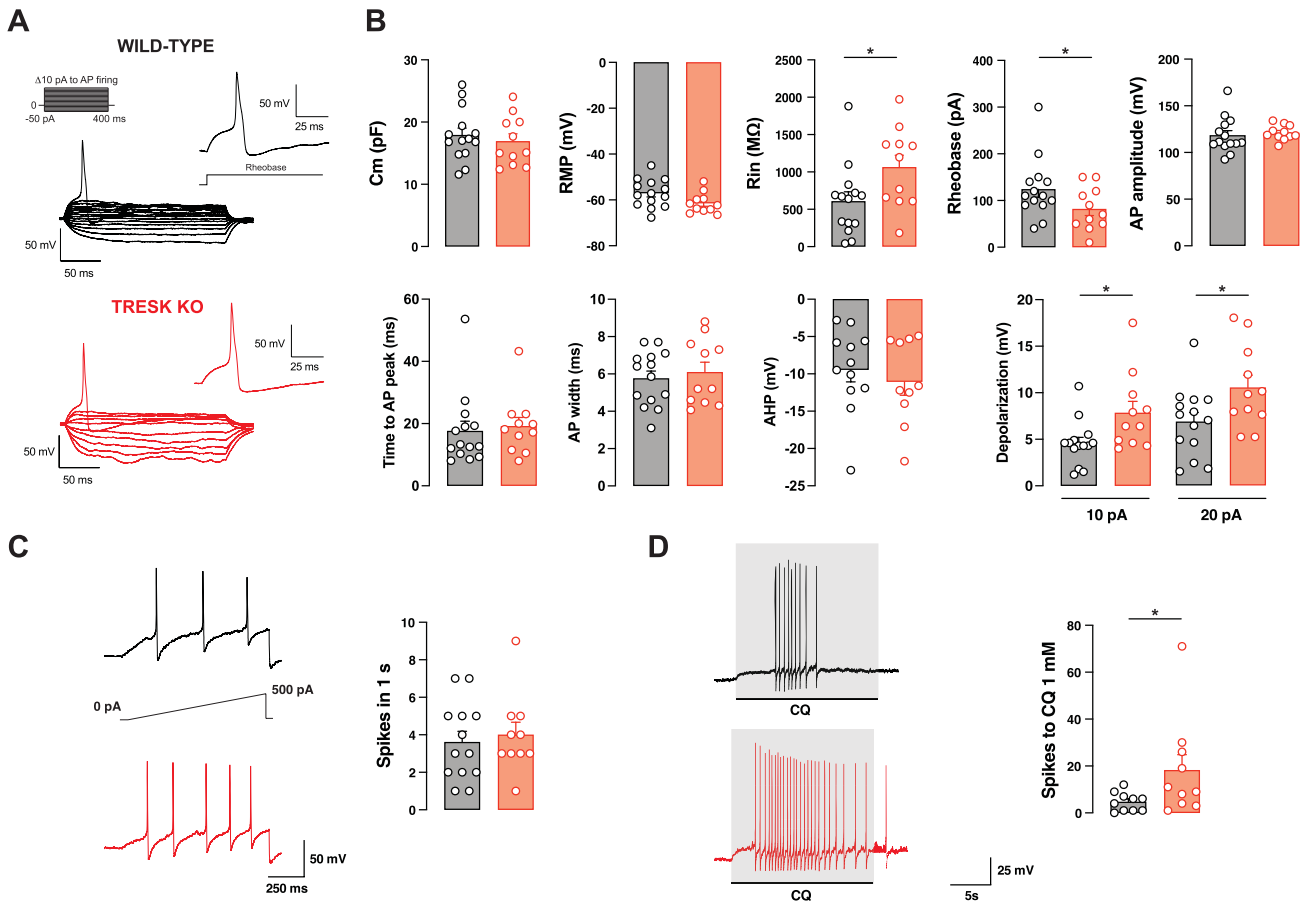


Figure 3. *MrgprA3*⁺ sensory neurons lacking TRESK exhibit increased excitability. (A) Representative whole-cell current-clamp recordings from primary cultures of *MrgprA3*⁺ sensory neurons obtained from *MrgprA3*^{tdTomato}; *TRESK*^{+/+} (left, top) and *MrgprA3*^{tdTomato}; *TRESK*^{-/-} (left, bottom) mice. Hyperpolarizing or depolarizing 400 ms current pulses in 10 pA increments from -50 pA to AP firing (Rheobase) were used. Inset: Magnification of the AP elicited at rheobase. (B) Quantification of the electrophysiological parameters analyzed in *MrgprA3*⁺ sensory neurons from wild-type (grey bars, n = 14) and TRESK knockout (KO) (red bars, n = 11) animals. Mean membrane capacitance (C_m) and resting membrane potential (RMP) from neurons recorded are shown. Whole-cell input resistance (R_{in}) was calculated from the -50 pA current pulse. Rheobase was measured using 400 ms depolarizing current pulses in 10 pA increments. Action potential amplitude was measured from the RMP to the AP peak. Time to AP peak was measured from the beginning of the depolarizing pulse to AP peak. Action potential duration/width was measured at 80% of the AP amplitude. Afterhyperpolarization (AHP) was measured from RMP. Depolarization induced by +10 and +20 pA subthreshold stimuli was measured from 400 ms depolarizing current pulses. (C) Intrinsic neuronal excitability was measured as the number of AP fired in response to a depolarizing ramp from 0 to 500 pA in 1 second from RMP (left). (D) Neuronal excitability to a pruritogenic stimulus was measured as the number of spikes fired in response to bath application of chloroquine (CQ, 1 mM; n = 10 for each genotype) for 20 seconds. Data are presented as mean ± SEM. Statistical differences between groups are shown as * $P < 0.05$, unpaired 2-tailed Student *t*-test. AP, action potential; TRESK, TWIK-related spinal cord K^+ channel.

($P = 0.512$). A small tendency to a more hyperpolarized RMP was observed in KO neurons but did not reach statistical significance ($P = 0.058$). Although a removal of a leak conductance would depolarize the cell, other compensatory mechanisms might compensate this and a possible effect of TRESK removal on RMP needs to be further studied with a larger number of recordings. Nevertheless, a previous study did not show significant differences, either.⁶ On the contrary, differences in input resistance and rheobase agree with a reduced potassium conductance, thereby facilitating neuronal depolarization and AP firing. To assess the contribution of potassium currents in the range of membrane potentials between resting and AP threshold, we measured the neuronal depolarization to subthreshold stimuli (+10 and +20 pA), which rendered significant larger depolarizations in neurons from TRESK KO animals (Fig. 3B). In addition, when subjected to a depolarizing ramp, KO neurons exhibited a trend towards firing a greater number of spikes (4.00 ± 0.67 ; n = 10; Fig. 3C) compared with their WT counterparts (3.62 ± 0.57 ; n = 13), although this difference did not reach statistical significance ($P = 0.332$). However, upon stimulation with CQ (1 mM),

neurons lacking TRESK fired significantly more spikes (18.20 ± 6.63 ; n = 10; $P < 0.05$; Fig. 3D) than those expressing the channel (6.82 ± 2.41 ; n = 11). This can explain why pruritic stimuli might lead to a heightened activation of the pathway.

3.4. TRESK delays and reduces chronic itch

In addition to systemic and neuropathic conditions, several dermatological conditions contribute significantly to itch, including psoriasis, dry skin (xerosis), and atopic or allergic dermatitis.^{39,49} As TRESK appears to modulate some forms of acute itch and *MrgprA3*-expressing neurons have been involved in chronic itch,^{37,66} we aimed to investigate whether the channel shapes the excitability of sensory afferents during chronic itch, potentially leading to an intensified sensation of spontaneous itch. To address this, we initially implemented a well-described mouse model of psoriasiform dermatitis induced by IMQ treatment, which closely resembles the human disease.^{17,42} Application of IMQ on the cheek skin over 7 consecutive days developed a psoriasis-like lesion accompanied by chronic spontaneous itch in WT animals. While both male and female mice exhibited evident

skin lesion and spontaneous itching, the number of scratching bouts was more pronounced in male mice, with female mice displaying a milder phenotype, consistent with previous reports.¹³ Consequently, subsequent studies using the IMQ model focused on male mice because of their more robust response, with data from female mice are provided in supplementary Figure 4 (<http://links.lww.com/PAIN/C222>).

Imiquimod treatment in male WT mice resulted in a progressive increase of spontaneous scratching bouts (day 2: 14.3 ± 3; day 3: 34.6 ± 8; day 4: 54.8 ± 13; *P* < 0.01 vs day 0) concurrent with the development of the skin lesion. Persistent itch remained elevated until the conclusion of the protocol (days 5-7: 41-45

scratching bouts, **Fig. 4A**). Vehicle-treated mice (vaseline) barely exhibited any significant itch response (scratching bouts ranged between 1 and 5; **Fig. 4A**), consistent with observations in basal conditions without any treatment. As expected, the IMQ-treated area displayed a characteristic psoriasis-like skin inflammation, characterized by thickening, scaliness, and erythema.⁴² A different cohort of mice (*n* = 5 mice per group) was used to collect histological samples from cheek skin and mRNA from ipsilateral trigeminal ganglion at day 4 of the treatment (maximum scratching time point). Compared to vehicle treatment, histological sections from cheek skin showed epidermal hyperplasia with a 2-fold increase in epidermal thickness (WT vehicle: 27.4 ±

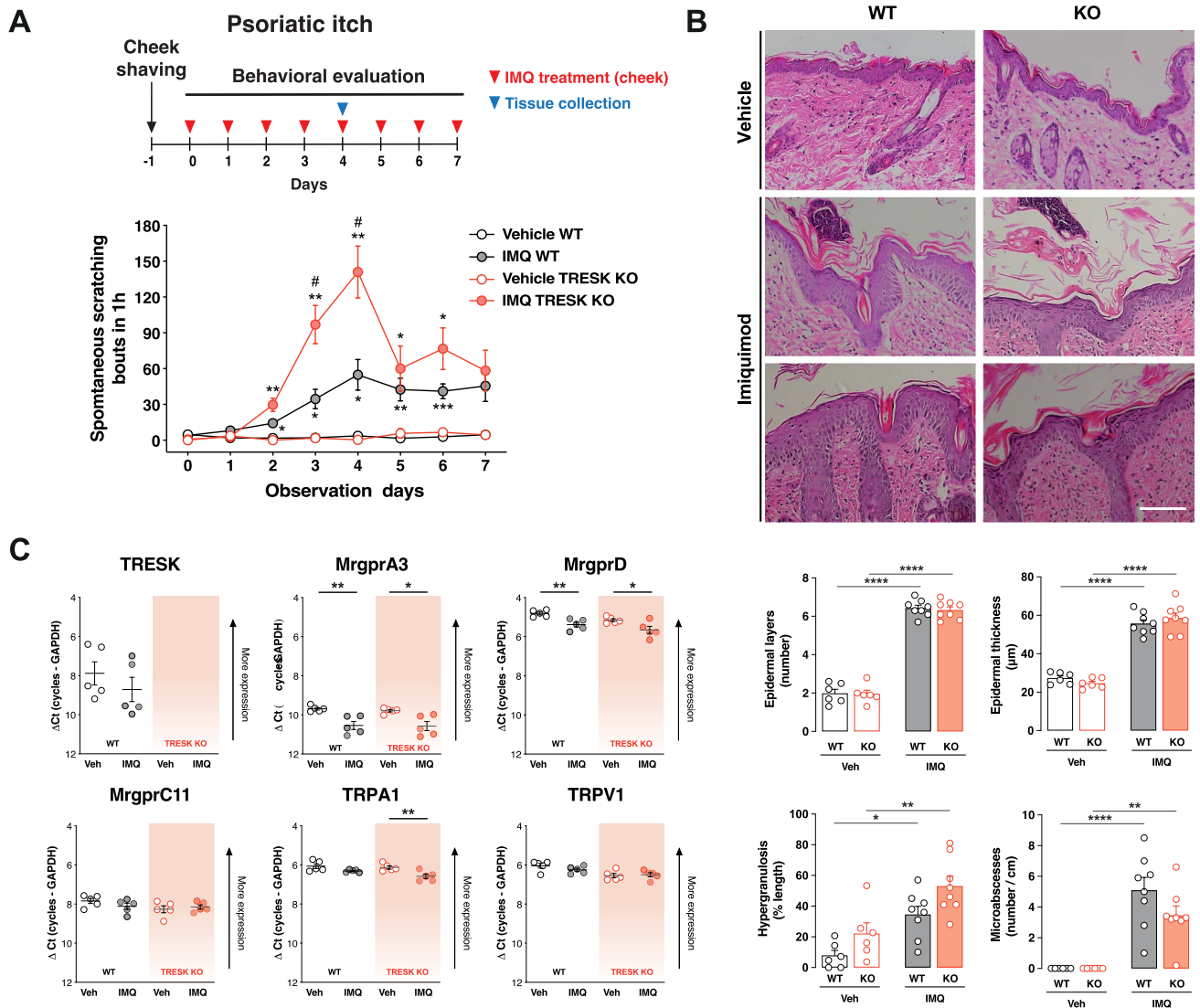


Figure 4. Psoriatic chronic itch is enhanced in the absence of TRESK. (A) Imiquimod (IMQ)-induced psoriasisform dermatitis model. *Top:* Time course for this model in the mouse cheek. *Bottom:* Time-dependent scratching bouts directed to the cheek skin from wild-type (WT) (vehicle, *n* = 8; IMQ, *n* = 15) and TRESK knockout (KO) male mice (vehicle, *n* = 4; IMQ, *n* = 8). Significant differences between groups are indicated as **P* < 0.05; ***P* < 0.01; ****P* < 0.001 vs vehicle WT/KO; #*P* < 0.05 IMQ WT vs IMQ KO; 2-way ANOVA followed by Bonferroni multiple comparisons tests. (B) *Top:* Imiquimod treatment on the cheek skin causes psoriasis-like skin lesions. Representative histological sections stained with hematoxylin and eosin from cheek skin on day 4 of treatment with vehicle (vaseline) or IMQ in WT or TRESK KO mice are shown. *Bottom:* Quantification of epidermal hyperplasia (as number of epidermal layers and epithelial thickness in µm), hypergranulosis (as % epidermal length with thickened stratum granulosum), and microabscesses (numbers/cm) in cheek skin samples from WT and TRESK KO mice. *n* = 6 (vehicle) and 8 (IMQ) per genotype. Scale bar = 100 µm. **P* < 0.05; ***P* < 0.01; *****P* < 0.0001 vs vehicle WT/KO; One-way ANOVA followed by Holm–Šidák multiple comparisons tests. (C) mRNA expression of TRESK, Mas-related G-protein-coupled receptor A3 (MrgprA3), MrgprD, MrgprC11, TRPA1, and TRPV1 in trigeminal sensory neurons from WT and TRESK KO mice at day 4 of IMQ treatment. Data obtained by quantitative polymerase chain reaction (PCR) show a significant decrease of MrgprA3 and MrgprD expression in WT and KO, and TRPA1 in KO animals, when comparing with vehicle-treated animals. However, no significant differences were observed between IMQ-treated WT and KO animals. Y-axis shows the ΔCt (number of cycles target - number of cycles GAPDH) for the different mRNAs. Notice that the Y-axis has been inverted to visually show that lower ΔCt numbers are indicative of a higher expression. Each dot represents a single animal (*n* = 5 ganglia per group and genotype). Statistical differences between groups are shown (**P* < 0.05, ***P* < 0.01 unpaired 2-tailed Student *t*-test). ANOVA, analysis of variance; GAPDH, glyceraldehyde 3-phosphate dehydrogenase; TRESK, TWIK-related spinal cord K⁺ channel.

1.2 μm vs WT IMQ: $55.7 \pm 2.0 \mu\text{m}$, $P < 0.0001$; **Fig. 4B**) and 3-fold increase in the number of skin epidermal layers (6.4 ± 0.2 vs 1.9 ± 0.2 , respectively; $P < 0.0001$; **Fig. 4B**). Imiquimod-treated skin also showed hypergranulosis (% epidermal length, vehicle: $7.8 \pm 3.4\%$ vs IMQ: $34.5 \pm 5.3\%$; $P < 0.05$) and a higher number of microabscesses (number/cm, vehicle 0.0 ± 0.0 vs IMQ: 5.1 ± 0.8 ; $P < 0.0001$; **Fig. 4B**). In animals lacking TRESK, a similar skin lesion was observed after IMQ treatment, and no significant differences were observed in histological sections when comparing epidermal thickness (WT: $55.7 \pm 2.0 \mu\text{m}$ vs KO: $58.5 \pm 2.6 \mu\text{m}$) or the number of skin epidermal layers between WT and KO animals treated with IMQ (6.4 ± 0.2 vs 6.3 ± 0.2 , respectively). Small differences that did not reach statistical significance were seen for hypergranulosis (% epidermal length WT: $34.5 \pm 5.3\%$ vs KO: $53.0 \pm 6.5\%$; $P = 0.074$) and the number of microabscesses (number/cm WT: 5.1 ± 0.8 vs KO: 3.5 ± 0.6 ; $P = 0.051$; **Fig. 4B**), suggesting that differences might exist at later time points. Nevertheless, in TRESK KO mice spontaneous itch was consistently higher compared to WT animals (analysis of variance $P < 0.0001$; IMQ-treated WT vs KO). Spontaneous itch developed earlier in the model and a larger number of scratching bouts were observed (day 2: 29.6 ± 5.5 scratching bouts; day 3: 97.0 ± 16.0 , $P < 0.05$; day 4: 141.0 ± 21.8 , $P < 0.05$; **Fig. 4A**) compared to IMQ-treated WT mice. Later, spontaneous scratching reached similar levels to those found in WT mice, suggesting that the absence of the channel promotes an earlier development of persistent spontaneous itch by facilitating pruriceptor activation and/or enhancing their excitability.

Trigeminal ganglion mRNA from the treated side (day 4) was extracted, and the expression of different membrane receptors and channels involved in itch detection and transduction was compared in the different groups (**Fig. 4C**). Imiquimod treatment did not induce a significant change in TRESK expression. However, both MrgprA3 and MrgprD showed a significant downregulation on their expression levels, both in WT and KO animals (**Fig. 4C**), suggesting that the skin lesion resulting from IMQ treatment may be inducing a deregulation of these membrane receptors. Similar effects on these receptors have been previously reported in DRGs after IMQ treatment in the back of WT animals.⁴² No significant changes in expression were observed for MrgprC11, TRPA1, or TRPV1, except a slight but significant decrease in TRPA1 expression in KO animals (**Fig. 4C**).

To further investigate the potential role of TRESK in itch associated with different dermatological conditions, we conducted a comparative analysis between WT and KO animals in 2 additional skin diseases models, allergic contact dermatitis (ACD) and dry skin (**Fig. 5**). In the ACD model, animals were initially sensitized through topical application of SADBE on the back skin and subsequently challenged with the compound in the mouse cheek a few days later, after established protocols.³⁷ After the first challenge, WT animals showed an increased number of scratching bouts directed to the treated area compared to vehicle or to values obtained previously to allergen application (vehicle: 1.9 ± 0.6 scratching bouts; prechallenge: 1.3 ± 0.5 ; first challenge: 18.4 ± 3.0 ; $P < 0.001$ vs prechallenge; **Fig. 5A**). Similar itching scores were observed during the second challenge with the allergen 1 day later (18.1 ± 3.3 ; $P < 0.01$ vs prechallenge values),

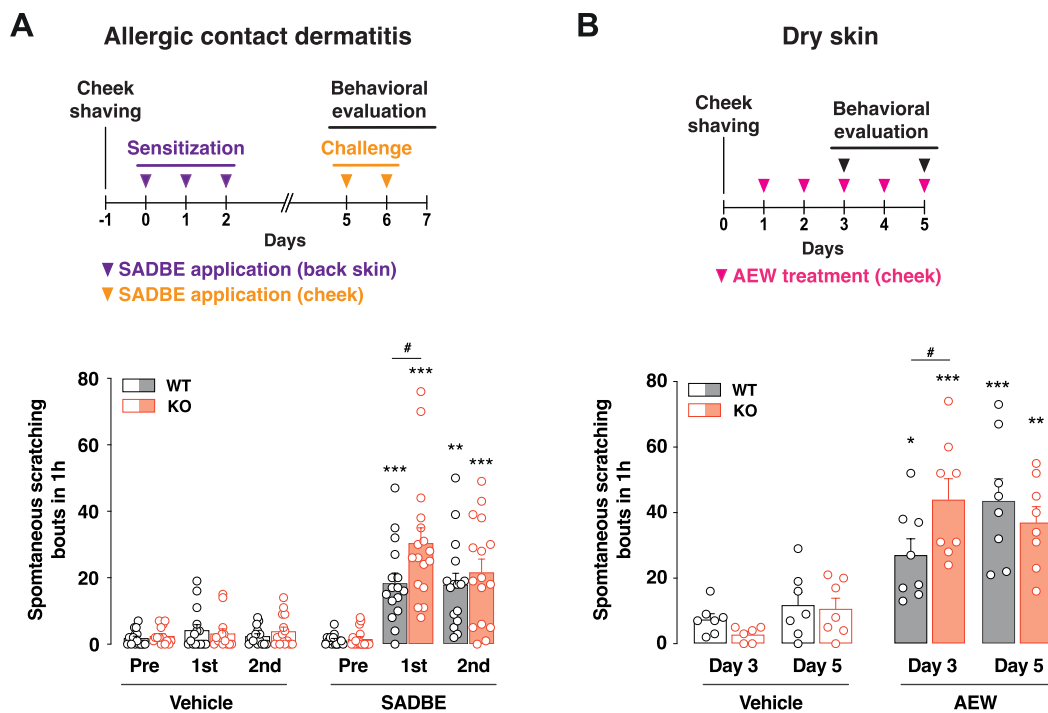


Figure 5. TRESK deletion also enhances chronic itch in other models of skin disease. (A) Allergic contact dermatitis model. *Top*: Time course for this model in the mouse cheek. Animals were initially sensitized with SADBE topical application in the back skin and then challenged with the compound in the mouse cheek a few days later. *Bottom*: quantification of the number of spontaneous scratching bouts directed to the cheek during 1 hour are plotted before (pre), 1 day after (first), and 2 days after (second) repetitive SADBE cheek application. Wild-type (WT) (vehicle, $n = 15$; SADBE, $n = 16$) and TRESK knockout (KO) mice (vehicle, $n = 15$; SADBE, $n = 17$). Significant differences between groups are shown as $**P < 0.01$; $***P < 0.001$ vs vehicle WT/KO 2-way ANOVA followed by Bonferroni multiple comparisons tests; $\#P < 0.05$ SADBE WT vs KO; 2-way ANOVA followed by Bonferroni multiple comparisons tests. (B) Dry skin model. *Top*: Time course for this model in the mouse cheek by repetitive application of acetone, ether, and water (AEW) to the cheek skin. *Bottom*: quantification of the number of spontaneous scratching bouts during 1 hour on day 3 and 5 are plotted. WT (vehicle, $n = 7$; AEW, $n = 8$) and TRESK KO mice (vehicle, $n = 7$; AEW, $n = 8$). Significant differences between groups are shown as $*P < 0.05$; $**P < 0.01$; $***P < 0.001$ vs vehicle WT/KO; $\#P < 0.05$ AEW WT vs KO 2-way ANOVA followed by Bonferroni multiple comparisons tests. ANOVA, analysis of variance; SADBE, squaric acid dibutyl ester; TRESK, TWIK-related spinal cord K^+ channel.

indicating that allergen sensitization resulted in a persistent effect upon each subsequent challenge with the allergic compound. In this model, KO animals displayed a more pronounced effect on the scratching score on the first day of the challenge (vehicle: 2.6 ± 0.7 scratching bouts; prechallenge: 1.6 ± 0.7 ; first challenge: 30.5 ± 4.5 ; $P < 0.001$ vs prechallenge; $P < 0.05$ vs WT mice; **Fig. 5A**), suggesting an enhanced activation of peripheral sensory afferents. On the second challenge, both WT and KO did not differ in the number of scratching bouts elicited (second challenge WT: 18.1 ± 3.3 ; KO: 21.7 ± 3.9), despite both groups presented significant itching compared to vehicle application.

A similar pattern was observed in the dry skin model, where repetitive application of acetone, ether, and water in the cheek led to the development of a skin lesion that induced robust itch behaviors on day 3 and beyond.⁶² As anticipated and compared to the vehicle (7.4 ± 1.7 scratching bouts), WT mice presented a substantial spontaneous pruritus on day 3 (27.1 ± 4.9 ; $P < 0.05$ vs vehicle; **Fig. 5B**), which further intensified at day 5 of treatment (43.6 ± 6.8 ; $P < 0.001$ vs vehicle). Similarly, to the ACD model, scratching induced by dry skin manifested earlier in the absence of TRESK channel, with maximum scratching values observed as earlier as day 3 (44.0 ± 6.4 ; $P < 0.001$ vs vehicle and $P < 0.05$ vs WT; **Fig. 5B**) and remaining consistent on day 5 (37.0 ± 4.8 ; $P < 0.01$ vs vehicle; ns vs WT). The similar pattern of early itch development across the 3 skin models suggests that the presence of the channel impedes or delays the development of persistent pruriceptor activation, and in its absence, sensory neurons display an enhanced susceptibility to activation by pruritic agonists.

3.5. Pharmacological activation of TRESK reduces itch

In contrast to histaminergic itch, which has a plethora of antihistaminergic drugs available, the ability to modulate certain forms of nonhistaminergic itch has long been pursued because of the lack of effective treatments or specific pharmacological compounds. Given that the absence of TRESK correlates with an enhancement of acute and chronic itch, both for therapeutic purposes and to further demonstrate the role of this channel, we evaluated whether its activation diminish scratching behavior, serving as a functional readout of itch sensitivity. Cloxyquin (Clx), an old antibacterial and antifungal drug used in *tuberculosis* treatment, has been identified as specific TRESK opener among the other 2-pore domain potassium channels,^{27,64} with an effect independent of the Ca^{2+} /calcieneurin-mediated potentiation of the channel current. Initially, we examined whether Clx could prevent CQ-induced acute itch in the cheek model. Intraperitoneal injection of Clx (50 mg/kg) or its vehicle (olive oil) administered 2 hours before the pruritic test did not induce any significant scratching in WT mice (**Fig. 6A**). In line with previous observations (**Fig. 2A**), CQ injection resulted in abundant scratching bouts directed to the cheek (61.4 ± 3.9 ; $P < 0.0001$ vs vehicle). Conversely, in animals previously injected with Clx, a significant reduction (57%) in the number of scratching bouts was obtained (35.1 ± 2.4 ; $P < 0.0001$ CQ + Clx vs CQ + veh; **Fig. 6A**), indicating that TRESK activation greatly reduced the number of observed scratchings. To confirm that the effect of Clx was because of TRESK channel activation and to rule out other potential side effects, we conducted the same experiment in mice lacking the channel. As previously demonstrated, in TRESK KO mice, CQ produced a significantly larger effect compared to WT animals (79.6 ± 8.2 scratching bouts vs 61.4 ± 3.9 ; $P < 0.05$; **Fig. 6A**), and this effect was not altered after Clx administration (74.4 ± 5.8 ; $P > 0.99$ vs CQ + veh). The significant difference

compared to WT mice ($P < 0.0001$) indicates that the channel must be present to obtain the therapeutic effect. We also tested whether a local application of Clx was able to reduce CQ-induced scratchings in the cheek. Neither a topical application of Clx, an intradermal coinjection with CQ, nor a Clx injection 30 minutes before CQ reduced the scratching bouts produced by CQ (Suppl Fig. 5, <http://links.lww.com/PAIN/C222>). These results suggest that either Clx is not being correctly absorbed or it does not reach sensory terminals in the skin. Alternatively, it is also possible that despite reaching the free nerve endings in the skin, TRESK effect is not significant there either because TRESK is not present in the nerve endings, or its effect is more prominent in the AP generation and transmission through the sensory fiber.

We next investigated whether the beneficial effect of TRESK activation extended to a model of chronic itch. Using the IMQ-induced of psoriatic itch model, we administered Clx or vehicle (i.p.) once daily from days 2 to 7, 2 hours before assessing scratching behavior. Vehicle injection yielded no significant effect, while, as anticipated, IMQ treatment in male mice led to a progressive increase in the number of scratchings events (**Fig. 6B**). In contrast, Clx treatment notably diminished spontaneous scratching over several consecutive days ($P < 0.01$; **Fig. 6B**), once again underscoring that the modulation of TRESK reduces the development of spontaneous itch in this model. As a control, TRESK KO mice developed IMQ-induced psoriatic itch, but no effect of the channel activator was observed (**Fig. 6C**).

4. Discussion

Channels active at subthreshold voltages, such as 2-pore domain potassium channels, are crucial for preventing excessive neuronal excitability by acting as a regulatory brake.³ Knocking out TRESK enhances neuronal excitability, increasing mechanical and cold pain,⁶ and channel downregulation postinjury, inflammation, or bone metastasis heightens sensory neurons excitability.^{31,57,65,67,71} Transcriptomic studies indicate notable TRESK expression in NP mouse sensory neurons and pruritogen receptor-enriched neurons in humans.^{8,12,30,34,38,53,58,59,68} We confirm significant coexpression of TRESK with MrgprD, MrgprA3, and MrgprC11 receptors in mice and with MrgprX1 in humans.³² This expression pattern implies TRESK's specific role in modulating the excitability of these neuronal subtypes. The enhanced effects of CQ in MrgprA3⁺ neurons and scratching behavior in TRESK KO animals confirm this hypothesis. Pruritogens acting on specific subpopulations were used to pharmacologically dissect this effect. Hrh1 is predominantly expressed in MrgprA3⁺ (NP2) and Nppb⁺ (NP3) neurons,⁴⁸ but histamine did not render significant differences in scratchings between WT and KO animals, suggesting that the combined effect in NP2/NP3 masks any enhanced response because of TRESK ablation. Indeed, after ablation of MrgprA3⁺ neurons with diphtheria toxin,¹⁶ mice still respond to histamine, indicating that histamine effects are not exclusively mediated by MrgprA3⁺ neurons. In fact, TRESK has a minimal expression in NP3 neurons and likely plays a minor role in their excitability.^{58,68} In agreement, LTC4, an agonist of Cyslr2 receptor specifically expressed in Nppb⁺ neurons,⁴⁸ did not produce observable differences in the scratching response between WT and KO animals. MrgprA3⁺ neurons have been further subdivided into NP2.1 and NP2.2.⁵⁸ To distinguish between both subpopulations, we used BAM8-22, whose receptor MrgprC11 is exclusively expressed in NP2.2 neurons.^{58,68} Despite NP2.2 neurons expressing MrgprA3 and TRESK at lower levels, the channel seems to play a minor role in these cells, as BAM8-22 induced

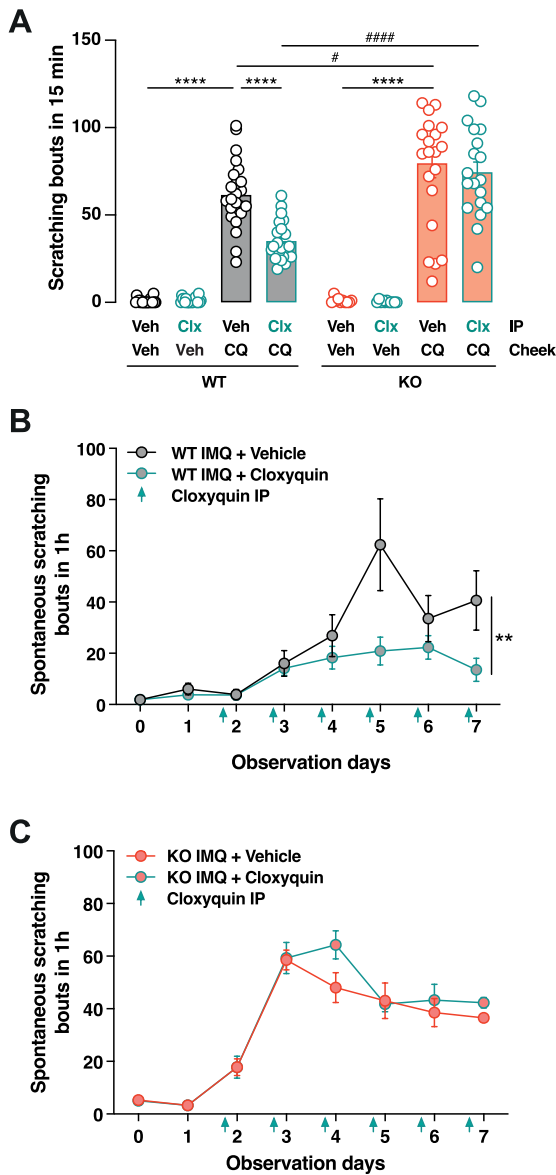


Figure 6. Pharmacological activation of TRESK reduces acute and chronic itch. (A) Acute itch produced by intradermal injection of chloroquine (CQ; 50 μ g) into the cheek was measured during 15 minutes, 2 hours after i.p. injection of cloxyquin (Clx; 50 mg/kg) or its vehicle (olive oil). Neither vehicle (olive oil) nor Clx produced significant scratching bouts compared to vehicle (phosphate buffered saline [PBS]) cheek injection. Chloroquine-induced scratchings were greatly reduced by pretreatment with Clx. The reducing effect of Clx was not observed in TRESK knockout (KO) animals, which corroborates the specific TRESK-mediated effect of the drug in wild-type (WT) animals. WT (vehicle/vehicle, $n = 21$; vehicle/Clx, $n = 21$; vehicle/CQ, $n = 24$; Clx/CQ, $n = 22$) and TRESK KO mice (vehicle/vehicle, $n = 10$; vehicle/Clx, $n = 11$; vehicle/CQ, $n = 21$; Clx/CQ, $n = 19$). Significant differences between groups of the same genotype are shown as: **** $P < 0.0001$. Differences between WT and KO groups are shown as # $P < 0.05$ and #### $P < 0.0001$. Two-way ANOVA followed by Bonferroni multiple comparisons tests. (B) Time-dependent scratching bouts in the imiquimod (IMQ)-induced psoriasiform dermatitis model in the cheek skin from WT male mice. Mice were injected with Clx (50 mg/kg; $n = 9$) or vehicle (olive oil; $n = 6$) 2 hours before observation as indicated by green arrows. A significant difference between treatments is shown as ** $P < 0.01$ 2-way ANOVA. (C) Time-dependent scratching bouts in the IMQ-induced psoriasiform dermatitis model in the cheek skin from KO male mice. Mice were injected with Clx (50 mg/kg; $n = 4$) or vehicle (olive oil; $n = 4$) 2 hours before observation as indicated by green arrows. No statistically significant differences were obtained. ANOVA, analysis of variance; TRESK, TWIK-related spinal cord K^+ channel.

similar scratching responses in WT and KO animals, which suggests an enhanced response to CQ mediated by NP2.1 neurons.

MrgprA3 is coupled to TRPA1 through a $G\beta\gamma$ signaling mechanism to allow an extracellular Ca^{2+} entry that is required for CQ-evoked itch.⁶¹ However, conflicting evidence arises from skin-nerve studies, where C-fibers activation by CQ remains unaffected in the presence of a TRPA1 blocker or in *Trpa1*-deficient mice but requires the participation of phospholipase $C\beta 3$.⁴¹ The chloride channel ANO1 also plays a role in transmitting Mrgpr-dependent itch in the periphery, as itch mediated by CQ, SLIGRL, or bilirubin is reduced in *Ano1*-deficient mice or in the presence of a ANO1 blocker.²¹ The precise mechanism for MrgprA3 receptor signaling remains to be fully elucidated, with potential involvement of TRPA1, ANO1, or other mechanisms such as TRPC3.⁵⁴ Interestingly, both TRPA1 and ANO1 expression is low in MrgprA3⁺ neurons, while ANO1 is highly expressed.^{54,66,68} Human MrgprX1 seems not linked to TRPA1 activation and instead, effects on neuronal excitability and itch might be related to direct modulation of tetrodotoxin-resistant sodium channels.⁵⁶ Our findings reveal that TRESK, in conjunction with other hyperpolarizing mechanisms, contributes to MrgprA3-dependent itch, likely by counteracting the depolarization induced by activation of TRPA1 and/or ANO1. Beyond membrane depolarization, calcium entry will slowly enhance TRESK current by calcineurin-dependent dephosphorylation of the intracellular loop serine cluster.⁹ Whether this also happens in humans via MrgprX1 receptors requires further investigation. Because of the multimodal capacity of MrgprA3⁺ sensory neurons, different agonists activate distinct signal transduction pathways to trigger pain or itch.⁴⁴ TRESK may be specifically associated with certain mechanisms, as evidenced by TRESK-deficient mice displaying increased itch in response to CQ but not to BAM8-22 and despite an important coexpression of MrgprC11 and TRESK. It is possible that both compounds activate different cell subtypes (NP2.1 and NP2.2) or initiate different signal transduction pathways.^{41,61}

Determinants of MrgprA3⁺ neurons' excitability are less clear compared to other neuronal subtypes, where specific ion channels play a crucial role in determining their unique firing.⁷⁰ Electrophysiological properties of MrgprA3⁺ neurons are consistent with previous findings.⁵² These neurons typically display a lower frequency of APs to depolarizing current injection compared to other sensory neurons, and repetitive firing is largely absent when exposed to suprathreshold stimuli (data not shown). However, MrgprA3⁺ neurons from TRESK-deficient mouse present larger depolarizations to subthreshold stimuli, a slightly increased firing upon current ramp injection and, more importantly, an increased firing response to CQ activation.

MrgprA3⁺ neurons play a significant role in the pathophysiology of chronic itch, as deletion of the Mrgpr-cluster or specific ablation of these neurons decrease itch in several dermatitis models.^{16,72} In addition, induction of chronic dermatitis with SADBE increases their excitability.³⁷ In the dry skin model, has been observed an increase in the number of MrgprA3⁺ peripheral fibers, DRG neurons, and MrgprA3 mRNA.⁴⁵ In these models, TRESK absence enhances spontaneous scratchings, suggesting that increased activation of MrgprA3⁺ neurons facilitate the development of the disease. These neurons also mediate the effects of endogenous pruritogens such as peptide GPR15L, which is increased in the skin of patients with psoriasis and atopic dermatitis.⁵⁵ GPR15L is released from inflamed keratinocytes and activates different Mas-related G-protein-coupled receptors in mast cells and sensory

neurons, including MrgprA3 (mice), MrgprX1, and X3 (humans).⁵⁵ Psoriasis is a chronic skin inflammatory disease characterized by hyperplasia, hyperkeratosis, and severe chronic itch.¹⁴ IMQ, a Toll-like receptor 7 agonist, is frequently used to induce psoriatic skin lesions and itch in mice, mimicking the human condition, especially in the B6 mouse strain.^{42,51} Mice lacking TRESK exhibit an earlier onset and a significant increase in the number of scratches, suggesting that the absence of the channel promotes neuronal activation and development of the itching associated psoriatic phenotype. As reported,¹³ IMQ skin treatment leads to a substantial increase in spontaneous scratching bouts in males, but only a minor increase in females, despite similar skin lesion and transcriptional IMQ signatures in both sexes.^{13,51} We noted that TRESK-deficient mice displayed even higher spontaneous itch behavior throughout the entire model. Although females exhibited a small number of spontaneous scratching bouts, all KO animals present higher spontaneous itch, albeit the differences were much smaller compared to males.

Despite not observing significant differences in the skin lesion between WT and KO mice at day 4 (when the maximum of scratching bouts was observed), it is possible that enhanced itch in KO animals facilitates an earlier development of the skin lesion. Hypergranulosis seems slightly increased in the KO mice, and it cannot be ruled out that, at later time points, some differences might be more evident. It remains to be determined whether the earlier onset of skin lesions in KO mice is because of increased neuronal activation or a more significant mechanical effect of scratchings. Elevated repetitive scratching could exacerbate skin lesions over time, and enhancing TRESK activation could potentially improve the condition. Furthermore, both WT and KO mice have a C57Bl/6N background, which exhibits a milder phenotype in the IMQ psoriasis model compared to that in C57Bl/6J mice, likely because of lower expression of IL-22 in the former.² Any differences between WT and KO mice might be more evident in C57Bl/6J mice, which presents a more aggravated dermatitis.

Imiquimod treatment regulates countless genes in the skin and in sensory neurons innervating the affected area, mirroring the processes observed in human psoriasis.^{42,50,51} We did not observe significant differences in mRNA expression of *trpa1*, *trpv1*, or *mrgprc11* in TG, when comparing IMQ-treated animals from both genotypes, suggesting that the expression of these proteins is not altered by the model. However, potential gene expression changes in neurons innervating the affected area might be masked by the overall expression of all TG neurons. Gene expression evaluation at a single-cell level in neurons innervating the affected area should provide a clearer view. As reported,⁴² no differences between genotypes were observed in IMQ-treated animals, but we noted a mRNA downregulation of MrgprA3 and MrgprD in both genotypes (vehicle vs IMQ), likely explained by the persistent activation. Imiquimod did not alter TRESK expressed in WT animals (compared to vehicle), which opens the possibility of using TRESK as a therapeutic target for chronic itch. Besides, IMQ has inhibitory effects on Kv, TREK-1, and TRAAK channels,²⁶ which we also observed on TRESK (not shown). This inhibition can contribute to chronic actions of IMQ, together with the immune and inflammatory mechanisms activated. Deleting TRESK produces a similar phenotypic pattern in chronic itch models, with enhanced pruritus during the initial days. This implies that, when present, TRESK limits sensory neurons activation, although these differences fade as each disease progresses.

Cloxyquin diminished the scratching episodes to CQ injection in WT, but not in KO mice, implying a specific effect on TRESK and unraveling the therapeutic potential of channel activation. Similarly,

in the IMQ chronic itch model, cloxyquin attenuated the pruritic phenotype only in WT. Optimizing therapeutic dosages and administration methods could improve the efficacy of pruritus suppression. These findings highlight the potential for developing TRESK activators as standalone or combination antipruritic agents for nonhistaminergic itch, potentially in conjunction with drugs targeting complementary mechanisms like Mrgpr inhibitors.

Conflict of interest statement

The authors have no conflicts of interest to declare.

Acknowledgments

Work supported by grant PID2020-119305RB-I00 (X.G. and N.C.), PID2023-148439OB-I00 (X.G.), PID2023-148332OA-I00 (G.C.), PID2020-114477RB-I00 (C.S.) funded by MCIN/AEI/10.13039/501100011033 of Spain; LF-OC-22-001114, Leo Foundation, Denmark (X.G.); NEA23-CRG184 National Eczema Association, USA (G.C.); 2021SGR00292 Generalitat de Catalunya (N.C.); AGORA: Advancing Guidelines with Original Research Achievements in pain, ERA-NET NEURON, EU (X.G.); Instituto de Salud Carlos III, Maria de Maeztu MDM-2017-0729 and CEX2021-001159-M (to Institut de Neurociències, Universitat de Barcelona).

Authors' contributions: Authors A.A.-B., A.C., G.C., N.C., and X.G. performed electrophysiological recordings in neurons and calcium imaging. J.L.-A., A.A.-B., I.P., A.C., and N.C. performed behavioral experiments. A.A.-B., I.P., and G.C. performed primary cell cultures. A.A.-B., J.L.-A., M.I.B., and A.P.-C. performed in situ hybridization and qPCR experiments. C.S., J.M.d.A., and A.A.-B. performed the histological experiments and analysis. J.L.-A., A.A.-B., C.S., N.C., G.C., and X.G. participated in the design of the study and performed the statistical analysis. G.C. and X.G. conceived the study, oversaw the research, and prepared the manuscript with help from all others. All authors read and approved the final manuscript.

The data that support the findings of this study are available from the corresponding author, X. Gasull, upon reasonable request.

Supplemental digital content

Supplemental digital content associated with this article can be found online at <http://links.lww.com/PAIN/C222>.

Supplemental video content

A video abstract associated with this article can be found on the PAIN Web site.

Article history:

Received 13 May 2024

Received in revised form 25 November 2024

Accepted 2 December 2024

Available online 6 March 2025

References

- [1] Andres-Bilbe A, Castellanos A, Pujol-Coma A, Callejo G, Comes N, Gasull X. The background K⁺ channel TRESK in sensory physiology and pain. *Int J Mol Sci* 2020;21:5206.
- [2] Bezdek S, Hdnah A, Sezin T, Mousavi S, Zillikens D, Ibrahim S, Ludwig RJ, Sadik CD. The genetic difference between C57Bl/6J and C57Bl/6N mice significantly impacts AldaraTM-induced psoriasiform dermatitis. *Exp Dermatol* 2017;26:349–51.

- [3] Busserolles J, Gasull X, Noël J. Potassium channels and pain. In: Wood JN, ed. *The Oxford handbook of the neurobiology of pain*. Oxford: Oxford University Press, 2019.
- [4] Callejo G, Castellanos A, Castany M, Gual A, Luna C, Acosta MC, Gallar J, Giblin JP, Gasull X. Acid-sensing ion channels detect moderate acidifications to induce ocular pain. *PAIN* 2015;156:483–95.
- [5] Castellanos A, Andres A, Bernal L, Callejo G, Comes N, Gual A, Giblin JP, Roza C, Gasull X. Pyrethroids inhibit K2P channels and activate sensory neurons: basis of insecticide-induced paraesthesias. *PAIN* 2018;159:92–105.
- [6] Castellanos A, Pujol-Coma A, Andres-Bilbe A, Negm A, Callejo G, Soto D, Noël J, Comes N, Gasull X. TRESK background K⁺ channel deletion selectively uncovers enhanced mechanical and cold sensitivity. *J Physiol* 2020;598:1017–38.
- [7] Cevikbas F, Lerner EA. Physiology and pathophysiology of itch. *Physiol Rev* 2020;100:945–82.
- [8] Chiu IM, Barrett LB, Williams EK, Strohlic DE, Lee S, Weyer AD, Lou S, Bryman G, Roberson DP, Ghasemlou N, Piccoli C, Ahat E, Wang V, Cobos EJ, Stucky CL, Ma Q, Liberles SD, Woolf C. Transcriptional profiling at whole population and single cell levels reveals somatosensory neuron molecular diversity. *eLife* 2014;3:e04660.
- [9] Czirájk G, Tóth ZE, Enyedi P. The two-pore domain K⁺ channel, TRESK, is activated by the cytoplasmic calcium signal through calcineurin. *J Biol Chem* 2004;279:18550–8.
- [10] Dong X, Dong X. Peripheral and central mechanisms of itch. *Neuron* 2018;98:482–94.
- [11] Enyedi P, Czirájk G. Molecular background of leak K⁺ currents: two-pore domain potassium channels. *Physiol Rev* 2010;90:559–605.
- [12] Flegel C, Schöbel N, Altmüller J, Becker C, Tannapfel A, Hatt H, Gisselmann G. RNA-seq analysis of human trigeminal and dorsal root ganglia with a focus on chemoreceptors. *PLoS One* 2015;10:e0128951.
- [13] Follansbee T, Zhou Y, Wu X, Delahanty J, Nguyen A, Domocos D, Carstens MI, Hwang ST, Carstens E. Signs of chronic itch in the mouse imiquimod model of psoriasisform dermatitis: sex differences and roles of TRPV1 and TRPA1. *Itch (Phila)* 2019;4:e25.
- [14] Greb JE, Goldminz AM, Elder JT, Lebwohl MG, Gladman DD, Wu JJ, Mehta NN, Finlay AY, Gottlieb AB. Psoriasis. *Nat Rev Dis Primers* 2016;2:16082.
- [15] Guo C, Jiang H, Huang CC, Li F, Olson W, Yang W, Fleming M, Yu G, Hoekel G, Luo W, Liu Q. Pain and itch coding mechanisms of polymodal sensory neurons. *Cell Rep* 2023;42:113316.
- [16] Han L, Ma C, Liu Q, Weng H-J, Cui Y, Tang Z, Kim Y, Nie H, Qu L, Patel KN, Li Z, McNeil B, He S, Guan Y, Xiao B, LaMotte RH, Dong X. A subpopulation of nociceptors specifically linked to itch. *Nat Neurosci* 2013;16:174–82.
- [17] Hawkes JE, Adalsteinsson JA, Gudjonsson JE, Ward NL. Research techniques made simple: murine models of human psoriasis. *J Invest Dermatol* 2018;138:e1–8.
- [18] Hill RZ, Morita T, Brem RB, Bautista DM. S1PR3 mediates itch and pain via distinct TRP channel-dependent pathways. *J Neurosci* 2018;38:7833–43.
- [19] Ikoma A, Steinhoff M, Ständer S, Yosipovitch G, Schmelz M. The neurobiology of itch. *Nat Rev Neurosci* 2006;7:535–47.
- [20] Kang D, Kim D. TREK-2 (K2P10.1) and TRESK (K2P18.1) are major background K⁺ channels in dorsal root ganglion neurons. *Am J Physiol Cell Physiol* 2006;291:C138–46.
- [21] Kim H, Kim H, Cho H, Lee B, Lu H-J, Kim K, Chung S, Shim W-S, Shin YK, Dong X, Wood JN, Oh U. Anoctamin 1/TMEM16A in pruriceptors is essential for Mas-related G protein receptor-dependent itch. *PAIN* 2022;163:2172–84.
- [22] Lafrenière RG, Cader MZ, Poulin J-F, Andres-Enguix I, Simoneau M, Gupta N, Boisvert K, Lafrenière F, McLaughlan S, Dubé M-P, Rankiniewicz MM, Ramagopalan S, Ansoorge O, Brais B, Sequeiros J, Pereira-Monteiro JM, Griffiths LR, Tucker SJ, Ebers G, Rouleau GA. A dominant-negative mutation in the TRESK potassium channel is linked to familial migraine with aura. *Nat Med* 2010;16:1157–60.
- [23] LaMotte RH, Dong X, Ringkamp M. Sensory neurons and circuits mediating itch. *Nat Rev Neurosci* 2014;15:19–31.
- [24] LaPaglia DM, Sapio MR, Burbelo PD, Thierry-Mieg J, Thierry-Mieg D, Raithel SJ, Ramsden CE, Iadarola MJ, Mannes AJ. RNA-Seq investigations of human post-mortem trigeminal ganglia. *Cephalalgia* 2018;38:912–32.
- [25] Le Pichon CE, Chesler AT. The functional and anatomical dissection of somatosensory subpopulations using mouse genetics. *Front Neuroanat* 2014;8:21.
- [26] Lee J, Kim T, Hong J, Woo J, Min H, Hwang E, Lee SJ, Lee CJ. Imiquimod enhances excitability of dorsal root ganglion neurons by inhibiting background (K2P) and voltage-gated (Kv)1.1 and Kv1.2 potassium channels. *Mol Pain* 2012;8:2.
- [27] Lengyel M, Dobolyi A, Czirájk G, Enyedi P. Selective and state-dependent activation of TRESK (K2P 18.1) background potassium channel by cloxyquin. *Br J Pharmacol* 2017;174:2102–13.
- [28] Liu Q, Tang Z, Surdenikova L, Kim S, Patel KN, Kim A, Ru F, Guan Y, Weng H-J, Geng Y, Undem BJ, Kollarik M, Chen ZF, Anderson DJ, Dong X. Sensory neuron-specific GPCR Mrgpr3 are itch receptors mediating chloroquine-induced pruritus. *Cell* 2009;139:1353–65.
- [29] Liu Q, Sikand P, Ma C, Tang Z, Han L, Li Z, Sun S, Lamotte RH, Dong X. Mechanisms of itch evoked by β -alanine. *J Neurosci* 2012;32:14532–37.
- [30] Mantioti S, Lehmann R, Flegel C, Vogel F, Hofreuter A, Schreiner BSP, Altmüller J, Becker C, Schöbel N, Hatt H, Gisselmann G. Comprehensive RNA-seq expression analysis of sensory ganglia with a focus on ion channels and GPCRs in trigeminal ganglia. *PLoS One* 2013;8:e79523.
- [31] Marsh B, Acosta C, Djouhri L, Lawson SN. Leak K⁺ channel mRNAs in dorsal root ganglia: relation to inflammation and spontaneous pain behaviour. *Mol Cell Neurosci* 2012;49:375–86.
- [32] Meixiong J, Dong X. Mas-related G protein-coupled receptors and the biology of itch sensation. *Annu Rev Genet* 2017;51:103–21.
- [33] Mishra SK, Hoon MA. The cells and circuitry for itch responses in mice. *Science* 2013;340:968–71.
- [34] Nguyen MQ, Wu Y, Bonilla LS, von Buchholtz LJ, Ryba NJP. Diversity amongst trigeminal neurons revealed by high throughput single cell sequencing. *PLoS One* 2017;12:e0185543.
- [35] Patel KN, Dong X. An itch to be scratched. *Neuron* 2010;68:334–39.
- [36] Pettingill P, Weir GA, Wei T, Wu Y, Flower G, Lalic T, Handel A, Duggal G, Chintawar S, Cheung J, Arunasalam K, Couper E, Haupt LM, Griffiths LR, Bassett A, Cowley SA, Cader MZ. A causal role for TRESK loss of function in migraine mechanisms. *Brain* 2019;142:3852–67.
- [37] Qu L, Fan N, Ma C, Wang T, Han L, Fu K, Wang Y, Shimada SG, Dong X, LaMotte RH. Enhanced excitability of MRGPRA3- and MRGPRD-positive nociceptors in a model of inflammatory itch and pain. *Brain* 2014;137(pt 4):1039–50.
- [38] Ray P, Torck A, Quigley L, Wangzhou A, Neiman M, Rao C, Lam T, Kim JY, Kim TH, Zhang MQ, Dussor G, Price TJ. Comparative transcriptome profiling of the human and mouse dorsal root ganglia: an RNA-seq-based resource for pain and sensory neuroscience research. *PAIN* 2018;159:1325–45.
- [39] Roh YS, Choi J, Sutaria N, Kwatra SG. Itch: epidemiology, clinical presentation, and diagnostic workup. *J Am Acad Dermatol* 2022;86:1–14.
- [40] Royal P, Andres-Bilbe A, Ávalos Prado P, Verkest C, Wdziekonski B, Schaub S, Baron A, Lesage F, Gasull X, Levitz J, Sandoz G. Migraine-associated TRESK mutations increase neuronal excitability through alternative translation initiation and inhibition of TREK. *Neuron* 2019;101:232–45.e6.
- [41] Ru F, Sun H, Jurcakova D, Herbtsomer RA, Meixiong J, Dong X, Undem BJ. Mechanisms of pruritogen-induced activation of itch nerves in isolated mouse skin. *J Physiol* 2017;595:3651–66.
- [42] Sakai K, Sanders KM, Youssef MR, Yanushefski KM, Jensen L, Yosipovitch G, Akiyama T. Mouse model of imiquimod-induced psoriatic itch. *PAIN* 2016;157:2536–43.
- [43] Salvatierra J, Diaz-Bustamante M, Meixiong J, Tierney E, Dong X, Bosmans F. A disease mutation reveals a role for Nav1.9 in acute itch. *J Clin Invest* 2018;128:5434–47.
- [44] Sharif B, Ase AR, Ribeiro-da-Silva A, Séguéla P. Differential coding of itch and pain by a subpopulation of primary afferent neurons. *Neuron* 2020;106:940–51.e4.
- [45] Shi H, Yu G, Geng X, Gu L, Yang N, Wang C, Zhu C, Yang Y, Yu L, Hu D, Yuan X, Lan L, Wu G, Tang Z. MrgprA3 shows sensitization to chloroquine in an acetone-ether-water mice model. *Neuroreport* 2017;28:1127–33.
- [46] Shiers SI, Sankaranarayanan I, Jeevakumar V, Cervantes A, Reese JC, Price TJ. Convergence of peptidergic and non-peptidergic protein markers in the human dorsal root ganglion and spinal dorsal horn. *J Comp Neurol* 2021;529:2771–88.
- [47] Shimada SG, LaMotte RH. Behavioral differentiation between itch and pain in mouse. *PAIN* 2008;139:681–7.
- [48] Solinski HJ, Kriegbaum MC, Tseng PY, Earnest TW, Gu X, Barik A, Chesler AT, Hoon MA. Nppb neurons are sensors of mast cell-induced itch. *Cell Rep* 2019;26:3561–73.e4.
- [49] Ständer S. Classification of itch. *Curr Probl Dermatol* 2016;50:1–4.
- [50] Swindell WR, Johnston A, Carbajal S, Han G, Wohn C, Lu J, Xing X, Nair RP, Voorhees JJ, Elder JT, Wang XJ, Sano S, Prens EP, DiGiovanni J, Pittelkow MR, Ward NL, Gudjonsson JE. Genome-wide expression profiling of five mouse models identifies similarities and differences with human psoriasis. *PLoS One* 2011;6:e18266.
- [51] Swindell WR, Michaels KA, Sutter AJ, Diaconu D, Fritz Y, Xing X, Sarkar MK, Liang Y, Tsoi A, Gudjonsson JE, Ward NL. Imiquimod has strain-dependent effects in mice and does not uniquely model human psoriasis. *Genome Med* 2017;9:24.

- [52] Tang M, Wu G, Wang Z, Yang N, Shi H, He Q, Zhu C, Yang Y, Yu G, Wang C, Yuan X, Liu Q, Guan Y, Dong X, Tang Z. Voltage-gated potassium channels involved in regulation of physiological function in MrgprA3-specific itch neurons. *Brain Res* 2016;1636:161–71.
- [53] Tavares-Ferreira D, Shiers S, Ray PR, Wangzhou A, Jeevakumar V, Sankaranarayanan I, Cervantes AM, Reese JC, Chamessian A, Copits BA, Dougherty PM, Gereau RW IV, Burton MD, Dussor G, Price TJ. Spatial transcriptomics of dorsal root ganglia identifies molecular signatures of human nociceptors. *Sci Transl Med* 2022;14:eabj8186.
- [54] Than JYL, Li L, Hasan R, Zhang X. Excitation and modulation of TRPA1, TRPV1, and TRPM8 channel-expressing sensory neurons by the pruritogen chloroquine. *J Biol Chem* 2013;288:12818–27.
- [55] Tseng PY, Hoon MA. GPR15L is an epithelial inflammation-derived pruritogen. *Sci Adv* 2022;8:eabm7342.
- [56] Tseng PY, Zheng Q, Li Z, Dong X. MrgprX1 mediates neuronal excitability and itch through tetrodotoxin-resistant sodium channels. *Itch (Phila)* 2019;4:e28.
- [57] Tulleuda A, Cokic B, Callejo G, Saiani B, Serra J, Gasull X. TRESK channel contribution to nociceptive sensory neurons excitability: modulation by nerve injury. *Mol Pain* 2011;7:30.
- [58] Usoskin D, Furlan A, Islam S, Abdo H, Lönnnerberg P, Lou D, Hjerling-Leffler J, Haeggström J, Kharchenko O, Kharchenko PV, Linnarsson S, Ernfors P. Unbiased classification of sensory neuron types by large-scale single-cell RNA sequencing. *Nat Neurosci* 2015;18:145–53.
- [59] Wangzhou A, McIvried LA, Paige C, Barragan-Iglesias P, Shiers S, Ahmad A, Guzman CA, Dussor G, Ray PR, Gereau RW, Price TJ. Pharmacological target-focused transcriptomic analysis of native vs cultured human and mouse dorsal root ganglia. *PAIN* 2020;161:1497–517.
- [60] Weir GA, Pettingill P, Wu Y, Duggal G, Ilie A-S, Akerman CJ, Cader MZ. The role of TRESK in discrete sensory neuron populations and somatosensory processing. *Front Mol Neurosci* 2019;12:170.
- [61] Wilson SR, Gerhold KA, Bifolck-Fisher A, Liu Q, Patel KN, Dong X, Bautista DM. TRPA1 is required for histamine-independent, Mas-related G protein-coupled receptor-mediated itch. *Nat Neurosci* 2011;14:595–602.
- [62] Wilson SR, Nelson AM, Batia L, Morita T, Estandian D, Owens DM, Lumpkin EA, Bautista DM. The ion channel TRPA1 is required for chronic itch. *J Neurosci* 2013;33:9283–94.
- [63] Wilson SR, Thé L, Batia LM, Beattie K, Katibah GE, McClain SP, Pellegrino M, Estandian DM, Bautista DM. The epithelial cell-derived atopic dermatitis cytokine TSLP activates neurons to induce itch. *Cell* 2013;155:285–95.
- [64] Wright PD, Weir G, Cartland J, Tickle D, Kettleborough C, Cader Z, Jerman J. Cloxyquin (5-Chloroquinolin-8-ol) is an activator of the two-pore domain potassium channel TRESK. *Biochem Biophysical Res Commun* 2013;441:463–8.
- [65] Wu S, Marie Lutz B, Miao X, Liang L, Mo K, Chang YJ, Du P, Soteropoulos P, Tian B, Kaufman AG, Bekker A, Hu Y, Tao YX. Dorsal root ganglion transcriptome analysis following peripheral nerve injury in mice. *Mol pain* 2016;12:1744806916629048.
- [66] Xing Y, Chen J, Hillel H, Steele H, Yang J, Han L. Molecular signature of pruriceptive MrgprA3+ neurons. *J Invest Dermatol* 2020;140:2041–50.
- [67] Yang Y, Li S, Jin ZR, Jing HB, Zhao HY, Liu BH, Liang YJ, Liu LY, Cai J, Wan Y, Xing GG. Decreased abundance of TRESK two-pore domain potassium channels in sensory neurons underlies the pain associated with bone metastasis. *Sci Signal* 2018;11:eaao5150.
- [68] Zeisel A, Hochgerner H, Lönnnerberg P, Johnsson A, Memic F, van der Zwan J, Häring M, Braun E, Borm LE, La Manno G, Codeluppi S, Furlan A, Lee K, Skene N, Harris KD, Hjerling-Leffler J, Arenas E, Ernfors P, Marklund U, Linnarsson S. Molecular architecture of the mouse nervous system. *Cell* 2018;174:999–1014.e22.
- [69] Zhang W, Shao W, Dong Z, Zhang S, Liu C, Chen S. Cloxiquine, a traditional antituberculosis agent, suppresses the growth and metastasis of melanoma cells through activation of PPAR γ . *Cell Death Dis* 2019;10:404.
- [70] Zheng Y, Liu P, Bai L, Trimmer JS, Bean BP, Ginty DD. Deep sequencing of somatosensory neurons reveals molecular determinants of intrinsic physiological properties. *Neuron* 2019;103:598–616.e7.
- [71] Zhou J, Yang CX, Zhong JY, Wang HB. Intrathecal TRESK gene recombinant adenovirus attenuates spared nerve injury-induced neuropathic pain in rats. *Neuroreport* 2013;24:131–6.
- [72] Zhu Y, Hanson CE, Liu Q, Han L. Mrgprs activation is required for chronic itch conditions in mice. *Itch* 2017;2:e9.
- [73] Zylka MJ, Dong X, Southwell AL, Anderson DJ. Atypical expansion in mice of the sensory neuron-specific Mrg G protein-coupled receptor family. *Proc Natl Acad Sci USA* 2003;100:10043–8.